UNIVERSITY OF CALIFORNIA
RIVERSIDE

Gas Phase Radical Migration in Peptides and Proteins

A Dissertation submitted in partial satisfaction
of the requirements for the degree of

Doctor of Philosophy

in

Chemistry

by

Benjamin Nathan Moore

June 2013

Dissertation Committee:
Dr. Ryan R. Julian, Chairperson
Dr. Cynthia Larive
Dr. Yinsheng Wang

The Dissertation of Benjamin Nathan Moore is approved:

_____

_____

_____

Committee Chairperson

University of California, Riverside

Acknowledgements

In the very distant future, all interesting and meaningful scientific questions may eventually be answered leaving no enigmas left to challenge the minds of young graduate students. I have been fortunate enough to live during a time when this is not the case, interesting scientific mysteries are plentiful, and new discoveries await those determined enough to seek them out. During my years as a graduate student I have pursued new scientific knowledge in the field of analytical chemistry and I am grateful to have had the support of family, friends, colleagues, and mentors. These individuals have both inspired me and enabled me to contribute to science in the ways that I have.

First and foremost I thank my wife Cindy for her love, support, and understanding during my entire graduate career. I also thank my parents, Ken and Pam, and my siblings, Hillary, Harry, and Allison for their love, support, and continued encouragement. I have been very lucky to have them by my side. I also thank my son Adrian with the hope that he may one day read this and be inspired to pursue his own interests, whatever they may be, to the furthest of his ability.

I thank my advisor Prof. Ryan Julian for all of his help and advice. Without his guidance, patience, and support none of my graduate work would have been possible. I also thank all previous and current members of the Julian group for their help and fruitful discussions. Specifically I would like to thank Tony Ly, Jolene Diedrich, Geoffrey Yeh, Helen Sun, and Zhenjiu Liu for their scientific advice and inspiration along with their friendship and support throughout the years. I also thank Vic Zhang, Yuanqi Tao, Omar Hamdy, H.J. Yang, and Nathan Hendricks for their continued support and wish them the best in the remainder of their studies. I thank my colleagues and fellow graduate students in the UCR Chemistry department for various helpful discussions, collaborations, and advice over the years. I also thank Prof. Stephen Blanksby for all of his help during collaborations with the Julian group. I thank Prof. Joe Loo for his help and for graciously allowing me to use the FT-ICR instrumentation at UCLA. I also thank Sheng Yin, Sabrina Benchaar, and Carly Ferguson for facilitating those experiments.

I thank the following institutions for funding: UC Riverside, the National Science Foundation, and the National Institutes of Health. The ECD data from Chapter 2 was collected using the FT-ICR in the lab of Joe Loo at UCLA. The work in Chapter 4 was performed in collaboration with Prof. Stephen Blanksby.

The work in Chapter 5 was performed in equal collaboration with Helen Sun, while Julie Hsu, Albert Lee, Gene Yoo, and Tony Ly performed a portion of the experimental work. Ryan R. Julian directed and supervised the research that forms the basis for this dissertation.

The text of this dissertation, in part or in full, is a reprint of the materials as they appear in the following publications:

Chpt. 2: Moore, B. N.; Ly, T.; Julian, R. R., *J. Am. Chem. Soc.* **2011,** *133,* 6997-7006.

Chpt. 3: Moore, B. N.; Julian, R. R., *PCCP* **2012,** *14*, 3148-3154.

Chpt. 4: Moore, B. N.; Blanksby, S. J.; Julian, R. R., *Chem. Commun.* **2009,** (33), 5015-5017.

Chpt. 5: Moore, B. N.; Sun, Q.; Hsu, J. C.; Lee, A. H.; Yoo, G. C.; Ly, T.; Julian, R. R., *J. Am. Soc. Mass. Spectrom.* **2011,** *23*, 460-468.

Dedication

To my wife, parents, and family,

for all of their encouragement and support.

ABSTRACT OF THE DISSERTATION

Gas Phase Radical Migration in Peptides and Proteins

by

Benjamin Nathan Moore

Doctor of Philosophy, Graduate Program in Chemistry
University of California, Riverside, June 2013
Dr. Ryan R. Julian, Chairperson

Radical chemistry represents a powerful set of reactions in which unstable odd electron species can undergo rapid and spontaneous chemical rearrangements. These reactions have recently found analytical use in the dissociation of peptides and proteins in mass spectrometry. In this dissertation, the factors controlling radical migration and dissociation are explored in detail through examination of model peptides and proteins by mass spectrometry and quantum mechanical calculation. Understanding the behavior of radicals in proteins is key to being able to further enhance their analytical usefulness.

Radicals already play an important role in electron capture dissociation (ECD) and electron transfer dissociation (ETD) mass spectrometry. When applied to peptides both gas phase dissociation methods yield nearly complete and uniform sequence coverage while retaining labile post-translational

modifications (PTMs). In contrast, a recently developed technique, radical directed dissociation (RDD), induces fragmentation at very specific locations in derivatized peptides and proteins which has proven useful in a variety of applications including the facile identification of PTMs. RDD provides very specific fragmentation and is complimentary to the broad uniform fragmentation provided by ECD/ETD. Despite these differences in observed dissociation patterns, ECD, ETD, and RDD are all driven by radical chemistry. This disparity in observed fragmentation can be explained by radical conversion and migration.

Radical migration in peptides typically occurs via hydrogen atom abstraction. In this manner radicals may travel to different sites within a molecule assuming the intermediate hydrogen atom transfer reactions are favorable both thermodynamically and kinetically. In this work, the thermodynamic factors, specifically the X-H bond dissociation energies (BDEs) of the 20 canonical amino acids, are determined by quantum mechanical calculation. These BDEs are then used to predict radical induced dissociation in peptides. UV-initiated gas phase peptide radicals are then used to examine radical migration experimentally. Radical induced fragmentation is observed at locations far from the initial radical site clearly indicating that radical migration occurs. Furthermore, good correlation exists between the BDE predicted and

experimentally observed radical migration patterns, regardless of charge polarity. It is also shown that radical migration pathways that do not yield immediate dissociation products can be tracked via ion-molecule reactions, specifically the reaction between a carbon centered radical and molecular oxygen gas.

The potential uses of radical chemistry in the examination of complex biomolecules such as proteins by mass spectrometry are numerous. The key to harnessing radicals for future analytical use lies in developing a deeper understanding of the thermodynamics and kinetics that control their behavior.

Table of Contents

List of Figures

List of Schemes

Chapter 1

Examining Radical Migration in Peptides and Proteins by Mass Spectrometry

1.1 Radicals in Biology

The covalent bond is one of the fundamental building blocks of chemistry and is fundamental to the construction of all organic molecules. Organic molecules formed by living organisms are referred to as biomolecules and they span a large range of complexity and size. Chemical reactions in biomolecules, and most organic molecules in general, usually involve the dissociation and formation of covalent bonds via the movement of electron pairs. In contrast, radical chemistry specifically refers to the creation and destruction of chemical bonds through the use of unpaired single electrons. Molecules containing unpaired electrons are typically unstable and can quickly react internally or with other nearby molecules to form more stable covalent bonds. In the case where a radical reacts with an electron from an electron pair to form a new covalent bond, the resulting molecule is still an odd-electron species and thus still contains a reactive radical. In the case where two radical species react with each other, the electrons recombine and the product is a stable even electron species. The ability of radicals to create and destroy bonds in this manner presents a wide

array of chemical reactions not easily accessible through the manipulation of paired electrons alone. This class of reactions has been utilized in modern synthetic chemistry to produce unique polymers and organic molecules via radical initiated reactions.[1,2,3] However, the use of radicals to perform important tasks is not new and has been necessary to the survival of living organisms for millennia.

Cellular organisms survive and function by creating proteins, which are complex macromolecules built from the polymerization of amino acids in a specific sequence. This sequence is built up by ribosomes according to the information encoded in the genetic material of the cell. From the canonical library of 20 different types of amino acids, proteins can be built to perform a wide range of biological tasks. Cellular growth, energy storage, movement, intercellular signaling, identification of extracellular objects, and reproduction are just a few examples of the processes performed by proteins.[4] The seemingly infinite span of protein functionality stems from both the chemical diversity of the amino acids used to produce the primary sequence along with the folding pattern of that amino acid chain into a 3-dimensional structure. The integral biological role that proteins fulfill mean that they are also key in the cause and progression of many diseases and cellular malfunctions; therefore it is important

to understand not only how proteins work correctly, but also how they can function incorrectly, i.e. change activity, become deactivated, destroyed, or otherwise damaged.[5]

Some proteins are capable of harnessing radicals to perform useful tasks. The ability to manipulate radicals in order to modify molecules can be a powerful tool for a biological system. For example, the protein ribonucleotide reductase uses radical chemistry to catalyze the reduction of ribonucleotides to deoxyribonucleotides.[6] This reaction is required to create the genetic material needed for cells to replicate, an essential process occurring in all living things. The innate ability of radicals to easily rearrange chemical bonds also leads to their use as destructive agents in cellular defense. In the human body, neutrophils are cells that envelop and destroy invading bacteria during an immune response. They do so by producing vesicles called phagosomes, which contain digestive enzymes and various reactive oxygen species (ROS) that can break down the captured bacteria.[7] Some ROS are free radicals that can wreak indiscriminate havoc by oxidizing and rearranging covalent bonds in any biomolecule within the phagosome. It has been proposed that ROS also play a role in the aging process[8], which has led to research into methods of limiting the damage caused by ROS outside of the necessary immune response. Antioxidants

are a class of compounds that can reduce this damage by sequestering the free radical away from other more important biomolecules. Living organisms have spent millions of years perfecting the complex relationship between antioxidants and ROS, a delicate balance between construction and destruction. Despite the energy, complexity, and inherent danger required to harness and use radicals, living organisms continue to do so in order to access the unique set of chemical reactions radicals are capable of performing.

1.2 Radicals in Mass Spectrometry

In addition to being a powerful tool in the arsenal of biological systems, radical chemistry has recently found a useful role in the analytical examination of biomolecules, namely in mass spectrometry based proteomics. Examination of peptides and proteins from a biological sample by mass spectrometry typically proceeds through one of two routes: top-down or bottom-up analysis.[9,10] In the top-down approach, proteins from an organism of interest are extracted and separated by chromatography. The proteins are then introduced into a mass spectrometer where each is isolated and fragmented in the gas phase. The resulting pieces are analyzed by mass to determine the identity and amount of the protein. The bottom-up approach instead involves solution phase fragmentation of the protein in a predictable fashion by enzymatic digest or

other means. The resulting peptides are then separated by chromatography and sequenced by dissociation in a mass spectrometer. From the observed peptide fragments and knowledge of the genome, the identity and amounts of the original proteins in the sample can be deduced.

Both of these approaches to proteomics rely heavily on having a reliable method to dissociate peptides and proteins in the gas phase. In the past, fragmentation of molecules in a mass spectrometer has been achieved by collision induced dissociation (CID) or infrared multiphoton photodissociation (IRMPD).[11,12] Both techniques slowly heat the molecule of interest, via multiple low energy collisions with a bath gas or absorption of infrared photons, respectively, until the weakest chemical bond is broken. Recently, electron capture dissociation (ECD)[13], electron transfer dissociation (ETD)[14], and radical directed dissociation (RDD)[15] have been shown to be very useful alternative methods for inducing dissociation of peptides and proteins in the gas phase. These methods differ from CID and IRMPD in that the creation of unstable radicals, instead of slow thermal heating, is used to break bonds in the molecule of interest. Typically the weakest bonds in positively charged gas phase peptides are the protonated backbone amide bonds, which upon dissociation, yield 'b' and 'y' type fragments.[16] Generic peptide backbone dissociation nomenclature is

shown in Scheme 1.1. Post-translational modifications (PTMs), which are chemical groups added to a protein after it has been synthesized, are also easily dissociated by slow heating methods.[17] In contrast, radical based techniques generally produce a/x and c/z fragmentation pairs. These methods are also able to retain labile PTMs such as phosphorylation and glycosylation.[13,18] These radical based dissociation techniques also produce numerous amino acid side chain fragmentation products, which are generally not observed in CID or IRMPD experiments. In some cases these side chain losses can be used to distinguish isobaric amino acids such as leucine and isoleucine.[19]

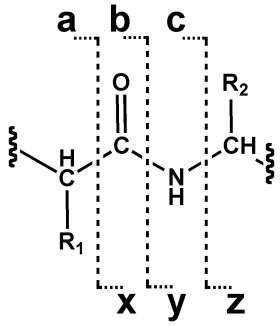

Scheme 1.1 Peptide backbone fragmentation nomenclature. Fragments a, b, and c contain the N-terminus while fragments x, y, and z contain the C-terminus.

Even though ECD/ETD and RDD are both radical based techniques, they produce vastly different results and thus have complimentary utility. A comparison of typical data acquired by these methods is shown in Figure 1.1. Simply from the observed dissociation patterns in Figure 1.1 it is clear that

radical chemistry can manifest itself in very different ways. In ECD, a thermal electron is "captured" by a protonated peptide cation in the gas phase. Although the exact mechanism remains unclear, the process forms a hydrogen-abundant radical that yields c/z type cleavage along the peptide backbone, along with side chain losses, as seen in Figure 1.1a. A hydrogen-abundant radical refers to a species having one more hydrogen atom than the molecular structure would normally have, a hydrogen-deficient radical having one less hydrogen atom, a subtle yet important difference which is explained in detail in Chapter 2. In contrast to ECD/ETD, peptides and proteins dissociated by RDD mainly yield a/x cleavage at aromatic residues, c/z fragmentation at serine, threonine, and the C-terminus, and side chain losses differing from those seen by ECD/ETD.[15] RDD refers to dissociation induced by hydrogen-deficient radicals. Hydrogen deficient radicals are created by methods such as homolytic dissociation of a chemical bond or single electron detachment from an anion.[20] In this work radicals for RDD were generated by gas phase UV-photodissociation of the carbon-iodine bond in iodo-tyrosine unless otherwise noted.[21]

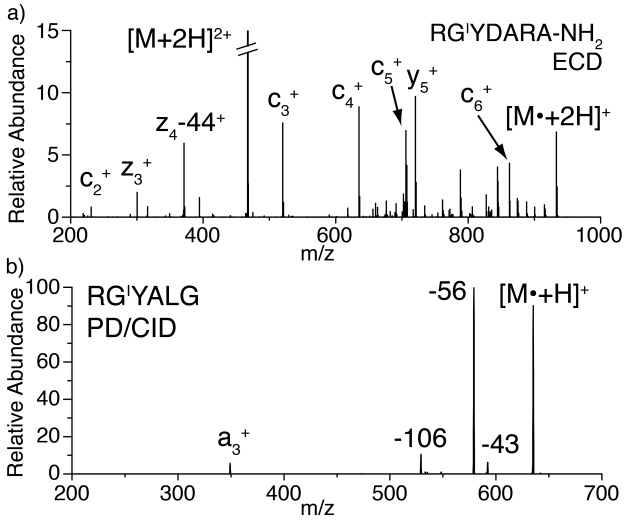

Figure 1.1 a) ECD fragmentation of the peptide RG^{I}YDARA-NH$_2$ showing typical c/z fragment formation. b) RDD fragmentation of the peptide RG^{I}YALG showing a/x fragmentation at the aromatic residue and large amounts of side chain loss.

In Chapter 2, the dissociation processes of ECD and RDD are explained and compared in detail. The mechanism underlying ECD has been heavily debated since its discovery, yet few studies have investigated the process from a purely radical chemistry point of view. It is shown in this work that although the backbone and side chain fragmentation observed in ECD is different from that seen in RDD, both are driven by radical chemistry and the two processes are more closely related than previously thought.

1.3 Factors Controlling the Behavior of Radicals

To further utilize radical directed dissociation of peptides and proteins by mass spectrometry it is necessary to understand what possible reactions they may cause. It has been previously discovered that radicals have the ability to

move between and within molecules by hydrogen atom abstraction. A generic form of this process is depicted in Scheme 1.2. An initiating radical interacts with an X-H bond to form a new bond and a new radical. (X = any atom in a covalent bond with hydrogen on the peptide) In this reaction the movement of the hydrogen atom and the radical are concomitant in opposite directions. Herein, this process will be referred to as radical migration.

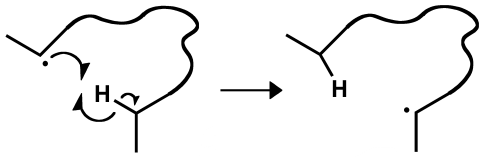

Scheme 1.2 General mechanism of radical migration via hydrogen atom abstraction.

Thermodynamics and kinetics are the important factors in predicting the likelihood of a radical migration reaction. A radical migration that is exothermic and results in a more stable radical is likely to occur spontaneously, assuming kinetic barriers such as improper alignment and steric hindrance are not present. On the other hand, a radical migration that is kinetically possible may be thermodynamically uphill meaning additional energy is required to push the radical to migrate to the position of higher instability. The kinetic factors involved in radical migration depend strongly on spatial structure, which for large biomolecules can be difficult to determine *a priori*. However, the thermodynamics of a radical migration, specifically the X-H bond dissociation

energies (BDEs), are easier to determine and are necessary for eventually being able to predict the favorability of any radical migration pathway. In Chapter 3 the BDEs of the 114 available hydrogen atoms on the 20 canonical amino acids are determined by quantum mechanical computation. From this set of energies, predictions can be made regarding where radicals are most likely to migrate to within peptides and proteins. The information presented in Chapter 3 will likely be important for expanding the current understanding of radical migration in proteins in the gas phase as well as in biological systems.

1.4 Radical Migration by Mass Spectrometry

Comparison between theoretically predicted and experimentally observed radical migration by mass spectrometry is the next logical step in understanding how radicals behave in gas phase peptide and protein ions. However, tracking radical migration by mass spectrometry can be a daunting challenge since intramolecular hydrogen atom transfers do not result in a change of mass or charge. Although the movement of a radical does not produce a mass shift, the reactivity of the radical changes dramatically depending on where it is located on an amino acid chain, as evident from the BDEs examined in Chapter 2. These differences in reactivity are exploited in Chapter 4 to probe gas phase radical migration on model peptides. Specifically, radical-radical recombination between

the peptide radical and molecular oxygen gas, a naturally occurring diradical species, results in different products depending on the site of the radical. For instance, an aromatic carbon radical on tyrosine undergoes a signature reaction resulting in immediate loss of •OH after addition of O_2. A similar reaction for a radical centered on an α-carbon primarily yields O_2 addition only with little observable loss of •OH. Coupled with deuterium labeling experiments, ion-molecule reactions with molecular oxygen are shown to be a very useful tool for tracking radical migration in peptides. Future experiments using other radical probe gases, i.e. nitric oxide, may be useful in further confirming the theoretically predicted radical migration pathways.

The correlation between theoretically predicted BDEs and experimentally observed radical migration is also examined in Chapter 5 through the analysis of a small library of negatively charged radical containing peptides. CID activation of these radical peptides shows that, regardless of charge, side chain loss and peptide backbone dissociation are governed by radical migration and BDEs. It is observed that radicals migrate from high BDE sites to low BDE sites to increase stability. Upon collisional activation, radical dissociation products from these low BDE sites are prominent while RDD products from high BDE sites are rarely observed. In addition, examination of the BDEs of anionic peptides predict a few

unique radical dissociation pathways which are not usually observed for cationic peptide radicals. These reactions are also examined and discussed in detail.

1.5 Future Utility of Radicals in Mass Spectrometry

Through evolutionary advances over time biological systems have come to harness the power of radical chemistry. Recently, mass spectrometrists have done the same by utilizing radicals to induce dissociation of peptides and proteins in the gas phase. The true potential of applying radical chemistry to mass spectrometry lies in the high reactivity of the odd electron species. If properly harnessed, radicals are capable of performing very specific reactions that are difficult or impossible to achieve otherwise. For example, the a/x and c/z fragments generated by ECD, ETD, and RDD are not usually observed by normal CID, and generally require high-energy collisions. RDD in particular is useful for generating a/x dissociation at specific residues, if proper chemical modifications are made. This specificity is very useful for identification of residues of interest and/or PTMs.

In other works, UV-photolabile modifications of cysteine[22], phosphoserine, phosphothreonine[18], tyrosine[21], tryptophan[23], histidine[24], lysine, and the N-terminus[25] have been shown thus far, but other residues may be accessible if suitable chemistry exists. For instance, the amino acid serine, 8.6% occurrence

rate in proteins[26], contains an alcohol group that offers little chemical reactivity. However, serine could be modified into a UV-labile chromophore by first phosphorylating with a nonspecific kinase followed by phosphate elimination and addition of an aromatic thiol. Proteins modified in such a manner could be quickly identified and sequenced in the gas phase by RDD. Another possibility is the modification of aspartic/glutamic acid or the C-terminus via ester activation and reaction with aromatic thiols or amines.

Any peptide modification resulting in a UV-labile chromophore has the potential to open up new applications for RDD. Expanding the available options for initial radical BDE and initial radical site will be key in designing new types of experiments. Increased specificity of dissociation is becoming an important goal for mass spectrometry based methods that attempt to examine larger and larger biomolecules. In UV initiated RDD, the specificity of dissociation is determined by the solution phase modification chemistry and gas phase radical migration. Assuming the solution phase chemistry and UV-photodissociation are extremely specific, the remaining factor is radical migration, in this case a potential problem. However, radical migration could be limited by choosing chromophores that yield relatively low BDE initial radicals. This may favor the

desired dissociation pathway and could open up new opportunities for obtaining specific information in very large biomolecules.

Organic synthesis might be able to create UV-labile chromophores that yield little radical migration, but it can also be used to enhance migration and manipulate the migration pathways. In Chapter 2 it is shown that alkylation of cysteine produces a side chain that is especially prone to radical induced dissociation, more so than any naturally occurring amino acid side chain. By building chemical moieties with high/low BDEs or high/low barrier dissociation pathways radical migration may be easily manipulated. For example, a hypothetical experiment might use radical migration to determine which parts of a protein interact in a protein-protein complex by initiating a radical on protein A and watching for RDD products from protein B. However, radical migration may be inhibited simply due to the fact that the amino acids involved in the potential migration pathways have unfavorable dissociation pathways, i.e. high BDEs. A way around this would be to add low BDE / low dissociation barrier side chain modifications to protein B, and to use a high BDE initial radical site on protein A, thus assisting any possible radical migration between the two proteins. Further study and understanding of radical migration may allow these types of experiments to become possible.

[1] Moad, G.; Rizzardo, E.; Thang, S. H., *Polymer* **2008,** *49* (5), 1079-1131.
[2] Braunecker, W. A.; Matyjaszewski, K., *Prog. Polym. Sci.* **2007,** *32* (1), 93-146.
[3] Hawker, C. J.; Wooley, K. L., *Science* **2005,** *309* (5738), 1200-1205.
[4] Barabasi, A. L.; Oltvai, Z. N., *Nat. Rev. Genet.* **2004,** *5* (2), 101-U15.
[5] Chiti, F.; Dobson, C. M., *Annu. Rev. Biochem* **2006,** *75*, 333-366.
[6] Reichard, P.; Ehrenberg, A., *Science* **1983,** *221* (4610), 514-519.
[7] Valko, M.; Leibfritz, D.; Moncol, J.; Cronin, M. T. D.; Mazur, M.; Telser, J., *Int. J. Biochem. Cell Bio.* **2007,** *39* (1), 44-84.
[8] Harman, D., *J. Gerontol.* **1956,** *11* (3), 298-300.
[9] McLafferty, F. W.; Breuker, K.; Jin, M.; Han, X. M.; Infusini, G.; Jiang, H.; Kong, X. L.; Begley, T. P., *FEBS J.* **2007,** *274* (24), 6256-6268.
[10] Bogdanov, B.; Smith, R. D., *Mass Spectrom. Rev.* **2005,** *24* (2), 168-200.
[11] Paizs, B.; Suhai, S., *Mass Spectrom. Rev.* **2005,** *24* (4), 508-548.
[12] Little, D. P.; Speir, J. P.; Senko, M. W.; Oconnor, P. B.; Mclafferty, F. W., *Anal. Chem.* **1994,** *66* (18), 2809-2815.
[13] Cooper, H. J.; Hakansson, K.; Marshall, A. G., *Mass Spectrom. Rev.* **2005,** *24* (2), 201-222.
[14] Syka, J. E. P.; Coon, J. J.; Schroeder, M. J.; Shabanowitz, J.; Hunt, D. F., *Proc. Natl. Acad. Sci. USA* **2004,** *101* (26), 9528-9533.
[15] Ly, T.; Julian, R. R., *J. Am. Chem. Soc.* **2010,** *132* (25), 8602-8609.
[16] Papayannopoulos, I. A., *Mass Spectrom. Rev.* **1995,** *14* (1), 49-73.
[17] Palumbo, A. M.; Tepe, J. J.; Reid, G. E., *J. Prot. Res.* **2008,** *7* (2), 771-779.
[18] Diedrich, J. K.; Julian, R. R., *Anal. Chem.* **2011,** *83* (17), 6818-6826.
[19] Kjeldsen, F.; Haselmann, K. F.; Sorensen, E. S.; Zubarev, R. A., *Anal. Chem.* **2003,** *75* (6), 1267-1274.
[20] Anusiewicz, I.; Jasionowski, M.; Skurski, P.; Simons, J., *J. Phys. Chem. A* **2005,** *109* (49), 11332-11337.
[21] Ly, T.; Julian, R. R., *J. Am. Chem. Soc.* **2008,** *130* (1), 351-358.
[22] Diedrich, J. K.; Julian, R. R., *Anal. Chem.* **2010,** *82* (10), 4006-4014.
[23] Knudsen, E. R.; Julian, R. R., *Int. J. Mass spectrom.* **2010,** *294* (2-3), 83-87.
[24] Sun, Q. Y.; Julian, R. R., *Rapid Commun. Mass Spectrom.* **2011,** *25* (15), 2240-2246.
[25] Ly, T.; Zhang, X.; Sun, Q. Y.; Moore, B.; Tao, Y. Q.; Julian, R. R., *Chem. Commun.* **2011,** *47* (10), 2835-2837.
[26] Echols, N.; Harrison, P.; Balasubramanian, S.; Luscombe, N. M.; Bertone, P.; Zhang, Z. L.; Gerstein, M., *Nucleic Acids Res.* **2002,** *30* (11), 2515-2523.

Chapter 2

Radical Conversion and Migration in Electron Capture Dissociation

2.1 Introduction

Electron capture dissociation (ECD) and the related method electron transfer dissociation (ETD) continue to be important methods for extracting information in mass spectrometry based proteomics experiments.[1-5] These techniques are employed to obtain sequence information from peptides and proteins. Importantly, highly labile post-translational modifications are typically preserved during ECD/ETD,[6] which simplifies identification relative to collisional activation methods.[7] Technological developments have also enabled ECD/ETD to be used in high throughput proteomic analyses, further increasing their utility.[8,9] Despite the value and popularity of ECD, the underlying mechanisms which dictate how fragmentation occurs are still not entirely clear and have been a subject for discussion over the last 10 years.[1,10,11,12]

Several of the mechanisms proposed for backbone dissociation in ECD proceed through an aminoketyl radical structure which dissociates into c and z$^{\bullet}$ ions as shown in Scheme 2.1. Formation of c/z$^{\bullet}$ ions in ECD is analytically useful due to the consistently high peptide sequence coverage when compared to b/y

ions generated by collision induced dissociation (CID). Although the formation of the aminoketyl radical and subsequent dissociation into backbone fragments has been studied previously in detail,[13,14] less attention has been given to other dissociation channels which are commonplace in ECD. For example, a variety of neutral losses from the charge reduced precursor ion are observed in ECD.[15-18] These neutral losses occur frequently and may provide additional insight into the mechanism of ECD which may not be apparent from examination of backbone dissociation alone. Indeed, alternatives to c/z• ion formation exist even for the aminoketyl radical itself, which can also potentially undergo radical migration as shown in Scheme 2.1b. It has also been postulated that a radical cascade mechanism may be responsible for some of the fragmentation observed in ECD.[19] Radical cascade mechanisms require an initial backbone c/z• dissociation and are similar in theory to dissociation observed from activation of z• product ions.[20,21]

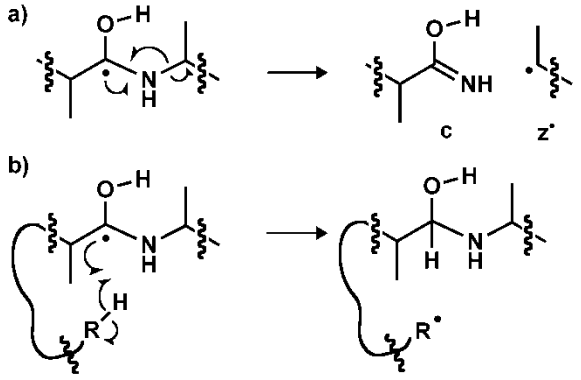

Scheme 2.1 a) Prototypical backbone dissociation into c/z• ions. b) Migration of the aminoketyl radical.

Neutral loss of amino acid sidechains is not exclusive to ECD but is also prevalent in experiments involving what are referred to as "hydrogen deficient" radical species. Hydrogen deficient radicals are distinct in that they have one less hydrogen atom than a peptide in a given charge state would typically have, i.e. $[(M-H)^{\bullet}+nH]^{n+}$. These radicals can be produced by various methods such as gas phase photodissociation (PD)[22,23], CID of anions[24], electron detachment dissociation[2526], electron induced dissociation[27], CID of nitroso- containing peptides[28], CID of peroxycarbamates[29], free radical initiated peptide sequencing (FRIPS)[30], dissociation of peptide-metal adducts,[31,32] and femtosecond laser pulses.[33] ECD itself also produces $c^{\bullet}$ and $z^{\bullet}$ type product ions which are hydrogen deficient radical species and behave as such.[15,34-39] Hydrogen deficient radical peptides generated by these methods typically yield amino acid sidechain losses and $a/x^{\bullet}$ backbone fragmentation when subjected to CID or radiative heating.[40] ECD on the other hand typically produces $c/z^{\bullet}$ fragments and sidechain losses, some of which are distinct to those observed in hydrogen deficient radical experiments.

A major hallmark of hydrogen deficient radical chemistry is radical migration, a process which allows the radical to travel to stable sites within the molecule.[41,42] In radical migration an initially formed hydrogen deficient radical

abstracts a neighboring hydrogen atom through space, thus quenching one radical and creating a new one as shown in Scheme 2.2a. Radical migration pathways allow a variety of sidechain losses and backbone dissociations to occur at sites distant from the location of the initial radical. We have previously proposed that radical migration pathways in peptides and proteins are determined by the bond dissociation energies (BDEs) of available hydrogens as well as the constraints imposed by the gas phase structure.[40] Migration is facilitated when the BDE of the radical acceptor site is comparable or lower than the BDE of the radical donor. Conformational constraints must also allow proper alignment of the donor and acceptor in order for migration to occur. Under conditions where the relative BDE difference is favorable and structural constraints are negligible, barriers to migration are predicted to be quite small.[42,43] Typically we have found that the flexibility available in moderately sized peptides minimizes structural constraints such that the BDEs become good qualitative predictors of radical mobility.[40] This is not the case in whole proteins where radical fragmentation is confined to spatially adjacent residues, although valuable structural information can be obtained in this fashion.[44]

At face value, backbone fragmentation and sidechain losses from the charge reduced precursor ion in ECD appear to be distinct from what is observed in

hydrogen deficient radical experiments because many of the products have been mass shifted. Formally, fragmentation in ECD is initiated from a "hydrogen abundant" radical species, i.e. $[(M+H^{\bullet})+nH]^{n+}$, which after charge reduction has one extra hydrogen atom relative to the canonical protonated species $[M+nH]^{n+}$. The hydrogen abundant product that is formed after electron capture becomes the initial structure leading to all observed ECD fragmentation. Electron capture, as proposed by McLafferty, Zubarev, and coworkers[1] in what is referred to as the Cornell mechanism, occurs directly at a protonated charge site resulting in a hydrogen abundant radical species. This species can then donate a hydrogen atom to a backbone carbonyl to form the aminoketyl radical and subsequently undergo $c/z^{\bullet}$ type fragmentation. Charge remote electron capture, as proposed by Turecek[45] and Simons[11,46], occurs by electron capture at a backbone carbonyl or disulfide to form an anionic species. Dissociation can then occur at the site of electron capture directly (Utah mechanism), or after proton transfer (Washington mechanism). Numerous charge remote capture pathways involving backbone or disulfide bond cleavage are frequently referred to collectively as the Utah-Washington mechanism. The Cornell and Washington mechanisms both involve conversion to a hydrogen deficient radical species; however, the possibility of radical migration within this species is not typically considered. For simplicity,

we will adopt the formalism of direct electron capture at charged sites to describe chemistry related to hydrogen deficient radical migration in the present manuscript. *It should be understood that, in theory, all of the chemistry that will be described could also be initiated by charge remote electron capture followed by proton transfer.* Determining the extent to which this might occur in actual ECD is beyond the scope of this paper.

It is important to point out that hydrogen abundant radical species can also undergo radical migration, but not by the hydrogen atom abstraction process previously described for hydrogen deficient radicals. Instead the excess hydrogen atom is transferred from the initial radical site to a hydrogen atom accepting site to form a new hydrogen abundant radical at that location as shown in Scheme 2.2b. In this case, the radical and hydrogen atom are collocated and move in the same direction which contrasts with hydrogen deficient migration where the hydrogen atom and radical migrate in opposite directions. This subtle difference in the mechanism of migration is an important characteristic in distinguishing hydrogen abundant and hydrogen deficient radical chemistry.

Hydrogen abundant radical migration should also not be confused with "radical conversion" where a hydrogen abundant radical is converted into a hydrogen deficient radical. An example is shown in Scheme 2.2c where the

aminoketyl radical, a hydrogen deficient product, is formed from the conversion of a hydrogen abundant precursor. Transfer of the abundant hydrogen from the charge reduced hypervalent amine transforms the backbone carbonyl into an alcohol thus converting the radical from hydrogen abundant to hydrogen deficient. A loss of a degree of saturation accompanies this process.

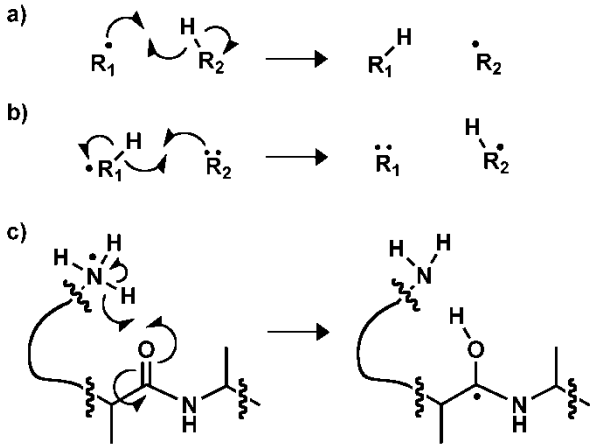

Scheme 2.2 Generic mechanisms of a) hydrogen deficient radical migration, where the radical and hydrogen atom exchange locations, b) hydrogen abundant radical migration, where the radical and hydrogen atom are collocated, and c) radical conversion from a hydrogen abundant to hydrogen deficient state.

In this paper we demonstrate that hydrogen deficient radical chemistry plays an important role in much of the dissociation that is observed in ECD. Statistical analysis of a large body of ECD data suggests that the hydrogen abundant species that are initially formed by electron capture quickly convert into hydrogen deficient radicals. This can occur via a variety of pathways; the most common pathways are outlined herein. Photodissociation experiments

designed to explore side chain dissociations observed in hydrogen deficient radical peptides are reported. These experiments confirm that hydrogen deficient chemistry can rationalize similar fragmentations observed in ECD, including selective fragmentation observed at disulfide bonds. Understanding the role that radical chemistry plays in ECD provides significant insight into the mechanisms which are responsible for both backbone and sidechain dissociation.

2.2 Experimental Section

The peptide RPPGYSPFR was purchased from American Peptide Co. (Sunnyvale, CA). This peptide was iodinated at tyrosine by a previously described method.[47] The carbon-iodine bonds of iodotyrosine containing peptides were photodissociated in the gas phase by transmitting fourth harmonic (266 nm) laser light, generated from a flash-pumped Nd:YAG laser (Continuum, Santa Clara, CA), through a quartz window on the rear vacuum flange of a modified LTQ linear ion trap (Thermo-Fisher, Waltham, MA) as previously described.[22] Alpha-methyl-cysteine was purchased from Nagase Co. (Osaka City, Japan), Fmoc protected[48], and acetamide protected. The peptides YVDIAIPCGNK and its alpha-methyl-cysteine derivative were synthesized by solid phase peptide synthesis.[48] S-cysteine-acetamide containing peptides were derived from cysteine containing peptides by reaction with an excess of iodoacetamide in

water in the dark at 40°C for 1 hour.[49] Dehydroalanine containing peptides were derived from phosphoserine containing peptides by reaction with $Ba(OH)_2$ solution at 40°C for 1 hour.[50] Disulfide bonded dipeptides were created by oxidizing two peptides each containing a single free cysteine in the presence of DMSO, 20% by volume in water.[51] Each of these products was purified separately on a C8 peptide purification column and diluted to a concentration of 5 μM before being electrosprayed.

Chemical structure and energy calculations were performed with the Gaussian 03 Ver. 6.1 Rev. D.01 software package (Gaussian, Inc., Wallingford, CT).[52] All calculations used the hybrid density functional theory B3LYP with the 6-31G(d) basis set unless otherwise stated. The bond dissociation energies (BDE) of the neutral aminoketyl radical, Gln, Glu, Asp, and Asn sidechain radicals were calculated by the isodesmic reaction method using the experimentally determined BDE of $H\text{-}CH_2OH$ (96.1 ± 0.2 kcal mol^{-1}) as a reference.[53] All other BDEs were calculated using appropriate reference energies. Transition states were determined by quasi-Newtonian synchronous transit (QST3) calculation and verified by visualization of the single imaginary frequency.[54]

Percentages of side chain loss in Table 2.1 were calculated based on analysis of the SwedECD database and are similar to those which have been previously

reported.[16] An algorithm was used which examined each peptide ECD spectrum in the database and looked for specific side chain losses by mass from the charge reduced species. The number of peptides containing the experimentally observed side chain loss and also contained the residue expected to generate the side chain loss were summed then divided by the total number of peptides containing the residue. Finally these values were converted to a percentage and compiled for all side chain losses in Table 2.1. Peptides containing amino acids with side chain losses that overlap by mass were excluded from the analysis when appropriate.

2.3 Results and Discussion

2.3.1 Evidence for Hydrogen Deficient Chemistry

It is first necessary to determine whether any of the numerous dissociation pathways observed in ECD are best explained by hydrogen deficient radical chemistry. For a statistically relevant source of ECD data, we will use the SwedECD database made publicly available by the Zubarev group.[16] SwedECD contains 11,491 ECD mass spectra of peptides derived from a tryptic digest of cell lysates. From this database we can extract trends relating formation of certain product ions with amino acid identity, sequence length, and a variety of other parameters. Specific sidechain losses from the charge reduced species in ECD have been previously investigated for their analytical utility in the differentiation

of isomeric sequences, improvement of database searching, and de novo sequencing.[16] In this work however sidechain loss will be used to investigate mechanistic details of ECD and its relation to hydrogen deficient radical chemistry. Only sidechain loss from the charge reduced parent ion in ECD is considered since this is the product ion that results directly from electron capture and may initially contain a hydrogen abundant radical. Sidechain losses from other products, such as $z^{\bullet}$ ions, have been examined previously and proceed through hydrogen deficient radical chemistry.[34] Table 2.1 shows sidechain losses that are typically observed in both hydrogen abundant and hydrogen deficient radical experiments. At first glance, most of the hydrogen deficient/abundant side chain losses in Table 2.1 appear to be different from each other and unrelated. However, closer inspection and consideration is warranted as will be detailed in the following sections.

Table 2.1 Partial List of Observed Neutral Sidechain Losses from the Charge Reduced Peptides in ECD and Observed Neutral Sidechain Losses from Hydrogen Deficient Radical Peptides

ECD Neutral Sidechain Losses				Hydrogen Deficient Radical Sidechain Losses		
Amino Acid	**Chemical Formula**	**Exact Mass**	**% Peptides With Loss**	**Amino Acid**	**Chemical Formula**	**Exact Mass**
Arg	$C_4H_{11}N_3$	101.0953	2.2	Arg	$C_4H_9N_3$	99.0796
Arg	CH_3N2	43.0296	14.3	Arg	$C_3H_8N_3$	86.0718
Asn	C_2H_5NO	59.0371	47.1 [a]	Asn	CH_2NO	44.0136
Asn	CH_2NO+NH_3	61.0401	13.8	Asp	CHO_2	44.9977
Asp	$C_2H_4O_2$	60.0211	60.4 [a]	Cys*	C_2H_4NO	58.0293
Asp	CHO_2+NH_3	62.0242	2.7	Cys*	C_2H_4NOS	90.0014
Cys*	C_2H_4NO	58.0293	88.8	Gln	C_2H_4NO	58.0293
Cys*	$C_2H_4NO+NH_3$	75.0558	19.9	Gln	C_3H_5NO	71.0371
Cys*	$C_2H_4NOS+NH_3$	107.0279	56.3	Glu	$C_2H_3O_2$	59.0133
Cys*	C_2H_5NO	59.0371	43.2 [a]	Glu	$C_3H_4O_2$	72.0211
Cys*	C_2H_4NOS	90.0014	42.3	His	$C_4H_4N_2$	80.0374
Gln	$C_2H_4NO+NH_3$	75.0558	14.8	His	$C_3H_3N_2$	67.0296
Gln	C_2H_5NO	59.0371	5.6 [a]	Ile	C_2H_5	29.0391
Gln	C_3H_5NO	71.0371	3.9	Ile	C_4H_8	56.0626
Gln	$C_3H_5NO+NH_3$	88.1000	0.3	Leu	C_4H_8	56.0626
Glu	$C_2H_3O_2+NH_3$	76.0393	21.3	Leu	C_3H_7	43.0584
Glu	$C_3H_4O_2+NH_3$	89.0471	6.7	Lys	C_3H_8N	58.0657
Glu	$C_2H_4O_2$	60.0211	1.0 [a]	Lys	C_4H_9N	71.0735
His	$C_4H_6N_2$	82.0531	38.4	Met	C_3H_6S	74.019
Ile	$C_2H_5+NH_3$	46.0651	7.2	Met	CH_3S	46.9955
Ile	$C_4H_8+NH_3$	73.0891	2.6 [a]	Met	C_2H_5S	61.0112
Ile	C_4H_8	56.0626	1.00 [a]	Ser	CH_2O	30.0106
Ile	C_2H_5	29.0391	0.7	Thr	C_2H_4O	44.0262
Leu	$C_4H_8+NH_3$	73.0891	11.9 [a]	Trp	C_9H_7N	129.0578
Leu	$C_3H_7+NH_3$	60.0849	11.6	Tyr	C_7H_6O	106.0419
Leu	C_4H_8	56.0626	4.7 [a]			
Leu	C_3H_7	43.0584	1.4			
Met	$C_3H_6S+NH_3$	91.0456	17.7			
Tyr	C_7H_8O	108.0575	3.5			

[a] Peptides containing other residues that exhibit the exact same sidechain loss by mass are excluding from these results. * Denotes S-cysteine-acetamide. % Peptides with Loss only considers peptides which contain the residue and is calculated by finding the percentage of peptides which upon ECD give the corresponding sidechain loss within ±0.01 Da.

Table 2.1 Observed sidechain losses in hydrogen abundant and hydrogen deficient radical experiments.

2.3.2 Leucine Radical Sidechain Loss

The sidechain loss of 56 Da from leucine is observed in both ECD experiments and when hydrogen deficient radicals are fragmented. However, simple observation of the same mass loss does not necessarily imply that the loss occurs via the same mechanism in both experiments, therefore likely hydrogen abundant and hydrogen deficient pathways for the loss of 56 are considered in Scheme 2.3. The loss of 56 Da represents the mass of nearly the entire side chain; however, as shown in Scheme 2.3a, homolytic cleavage of the appropriate bond would actually result in a loss of 57 Da. Therefore, any correct mechanism will require the transfer of a hydrogen atom from the sidechain to the peptide prior to dissociation. Hydrogen abundant dissociation typically involves attack by the excess hydrogen atom (see Scheme 2.2b), which is unlikely in the case of the leucine side chain due to the absence of favorable sites to receive the hydrogen atom. Furthermore, attack at the side chain would ultimately result in a loss of 58 Da as shown in Scheme 2.3b, not the required 56 Da. Similarly, hydrogen atom attack at the alpha position would result in a loss of 57 Da, which is not acceptable either. Hydrogen abundant radical chemistry does not therefore offer a palatable explanation for the observed loss. In contrast, hydrogen deficient

chemistry readily leads to this type of loss via the mechanism outlined in Scheme 2.3c.[40] If the initial hydrogen abundant parent ion underwent conversion to a hydrogen deficient species, then migration of that radical to the gamma position of leucine would provide the required hydrogen transfer. Subsequent beta dissociation would generate the observed loss of 56 Da. Consideration of all possible mechanisms suggests that this loss is actually generated by the same pathway in both ECD and hydrogen deficient radical experiments. Furthermore, it implies that significant conversion to a hydrogen deficient state capable of radical migration occurs within the charge reduced parent ion in ECD.

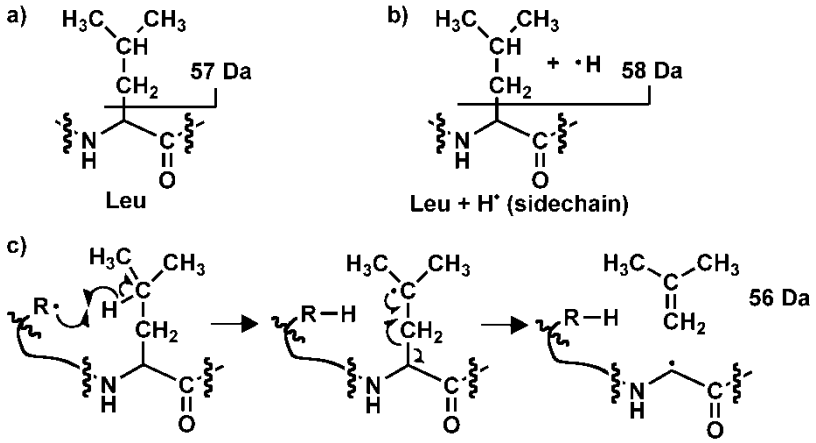

Scheme 2.3 Leucine side chain loss. a) Homolytic cleavage of the C_α – C_β bond results in 57 Da loss. b) Attack by hydrogen atom results in loss of 58 Da. c) Abstraction of the γ hydrogen yields the observed loss of 56 Da.

2.3.3 S-cysteine-acetamide sidechain loss and disulfide bond cleavage

Another sidechain loss observed in both ECD and hydrogen deficient radical experiments is the loss of the S-cysteine-acetamide sidechain. In the SwedECD

study, peptides were reacted with iodoacetamide to cap cysteine residues thus forming S-cysteine-acetamide and preventing any possible disulfide bond formation (this is commonly done in proteomics experiments). As seen in Table 2.1, peptides containing modified cysteine have a ~42% probability of producing a loss of 90 Da in ECD experiments. This loss is therefore highly favored in ECD. Hydrogen deficient radical peptides containing modified cysteine have not been investigated previously. In order to provide context for comparison, several peptides were treated with iodoacetamide to cap the cysteine, iodinated at tyrosine, and converted into a hydrogen deficient radicals by photoactivation. As shown in Figure 2.1a, collisional activation of [(CDPGYIGSR)•+H]+ yields a dominant loss of 90 Da. As discussed previously, radical migration is influenced by both relative BDEs and peptide structure. The results in Figure 1a likely result from structural factors which favor migration of the radical to cysteine; nevertheless, it is clear that the loss of 90 Da can be highly favored under proper conditions. It is anticipated that doubly protonated CDPGYIGSR will not have the same structure as the singly protonated ion, which should influence radical migration. Indeed, Figure 2.1b shows CID of the doubly charged peptide radical yields a loss of 90 Da, though several other dissociation channels are observed as well. The results in Figure 2.1 are similar to those obtained for several other

peptides and confirm that the loss of 90 Da from modified cysteine is a favorable dissociation channel in hydrogen deficient radical peptides.

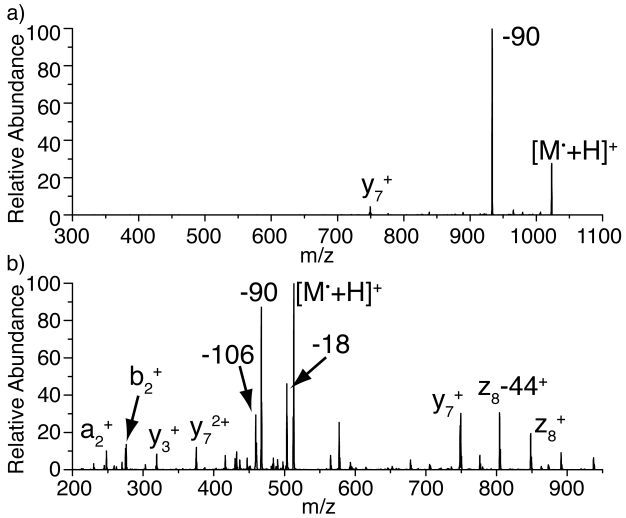

Figure 2.1 a) PD/CID of singly charged $[(cDPGYIGSR)^{\bullet}+H]^{+}$. b) PD/CID of doubly charged $[(cDPGYIGSR)^{\bullet}+2H]^{2+}$. Lower case 'c' denotes the amino acid S-cysteine-acetamide.

Possible mechanisms for the loss of 90 Da from modified cysteine are shown in Scheme 2.4. Homolytic cleavage of the C-S bond in S-cysteine-acetamide would indeed result in the observed 90 Da loss. There are two pathways which can lead to this loss. The first involves hydrogen atom attack at the β-carbon as shown in Scheme 2.4b. The β-carbon position in amino acids is not predicted to have a high hydrogen atom affinity because a pentavalent carbon intermediate is created, which mitigates the likelihood of this mechanism. Alternatively, a hydrogen deficient radical starting from the α-position of the amino acid is able to rearrange and produce the 90 Da sidechain loss as shown in Scheme 4c. The

α-position is known to stabilize hydrogen deficient radicals due to the captodative effect.[5153,56] The results in Figure 2.1 clearly demonstrate that the 90 Da loss mechanism in Scheme 2.4c is favorable; however, further experiments are needed to prove that the same pathway is operative in ECD. To probe this issue experimentally, two peptides with the sequence YVDIAIPcGNK were prepared, one of them containing an alpha methyl cysteine variant. The alpha methyl group should block the pathway outlined in Scheme 2.4c (because the abstracted hydrogen is replaced with a methyl group) while leaving the pathway in Scheme 2.4b open. The results in Figure 2.2a illustrate that the expected loss of 90Da is observed in the standard peptide. In Figure 2.2b however, the alpha methyl variant does not exhibit a loss of 90Da, confirming that this loss proceeds via the mechanism outlined in Scheme 2.4c in ECD experiments.

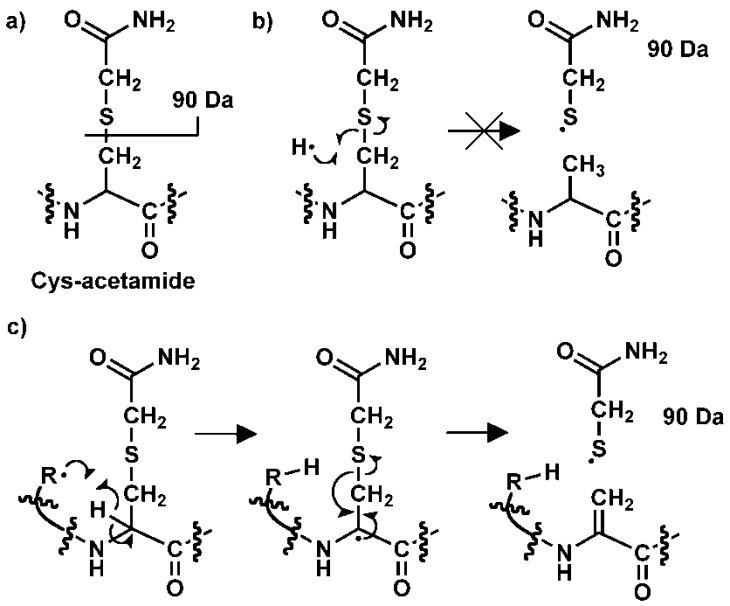

Scheme 2.4 S-cysteine-acetamide side chain loss. a) Homolytic cleavage of the C_β–S bond results in 90 Da loss. b) Hydrogen atom transfer to the β-carbon could produce the 90 Da loss. c) Abstraction of the alpha hydrogen yields the experimentally observed 90 Da loss.

If hydrogen deficient radicals access the α-positions of amino acids following electron capture, radical conversion, and migration, then why is dissociation at modified cysteine observed while other comparable side chain losses are not? The most plausible hypothesis relates to the stability of the products, which is known to influence transition state energies in hydrogen deficient radical dissociation. The BDEs for all possible side chain losses that can occur from the alpha radical initiation are shown in Figure 2.2c. The range of BDEs for all alpha radicals is highlighted in red.[53] Only the loss of modified cysteine yields a radical which is not considerably less stable than radicals in the alpha position. All other side chain losses are therefore predicted to be significantly endothermic and less

favorable. When taken as a whole, it is clear that consideration of the relevant energetics from a hydrogen deficient radical chemistry perspective explains both the favorable loss of 90 Da from modified cysteine and the absence of other equivalent side chain losses from the remaining amino acids.

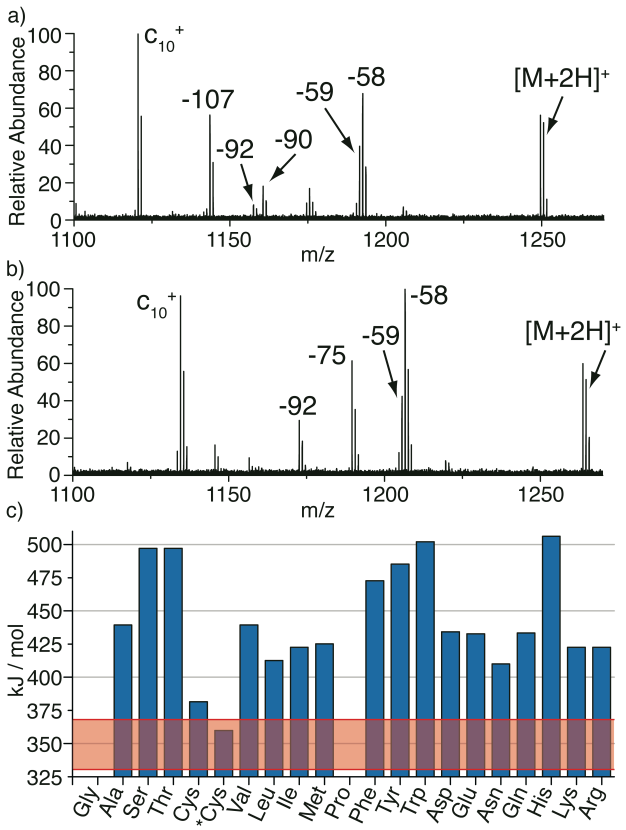

Figure 2.2 a) ECD spectrum of the peptide YVDIAIPcGNK. b) ECD spectrum of the peptide YVDIAIPc*GNK where c* denotes alpha-methyl-cysteine. c) BDEs of the products resulting from alpha radical driven sidechain dissociation from standard amino acids and the nonstandard amino acid S-cysteine-acetamide. The red region is the BDE range of amino acid alpha hydrogens.

2.3.4 Disulfide Bonds

The specific cleavage of disulfide bonds by ECD is a well-known process which is thought to occur via one of two pathways: direct electron capture into an antibonding orbital of the disulfide bond, or hydrogen atom attack at one of the sulfur atoms.[3,11] Both of these mechanisms may be occurring in ECD, but a hydrogen deficient radical pathway also exists and may contribute to the observed disulfide cleavage products. The singly disulfide bound complex resulting from combination of the peptides RPHERNGFTVLCPKN and VCYDKSFPISHVR (iodinated at tyrosine) was subjected to photodissociation to generate a hydrogen deficient radical system. Collisional activation of the radical product is shown in Figure 2.3a. Cleavage of the disulfide bond leads to the major products. Again, the highly dominant disulfide dissociation is likely due to favorable structural features which place the disulfide and nascent radical in close proximity. When the even electron peptide complex is subjected to CID, no disulfide dissociation is observed. For comparison, a similar experiment with peptides SLRRSSCFGGR and CDPGYIGSR (iodinated at tyrosine) is shown in Figure 2.3b. In this case, dissociation at the disulfide is less dominant and accompanied by related losses stemming from cleavage of the C-S bond adjacent to the disulfide. The hydrogen deficient pathways that lead to these products are

shown in Scheme 2.5. Cleavage of the disulfide bond can be initiated from attack at the β-position or directly at the disulfide.[57] In contrast, dissociation of the C-S bond is initiated from the more stable α-position. The data in Figure 2.3 clearly confirms that both pathways are possible in hydrogen deficient radical peptides. Both types of dissociation are also observed in actual ECD experiments.[3] Given that we have established that hydrogen deficient radicals are generated in ECD experiments, it is likely that some portion of the dissociation observed at disulfide bonds occurs via the pathways outlined in Scheme 2.5. The observed preference for dissociation at disulfide bonds in ECD may be due to the existence of multiple feasible fragmentation pathways.

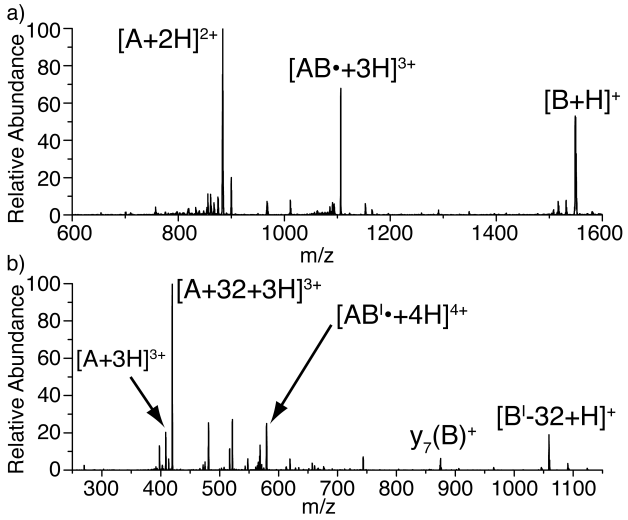

Figure 2.3 a) PD/CID of the disulfide bound peptides A: VCYDKSFPISHVR and B: RPHERNGFTVLCPKN and b) PD/CID of the disulfide bound peptides A: SLRRSSCFGGR and B: CDPGYIGSR.

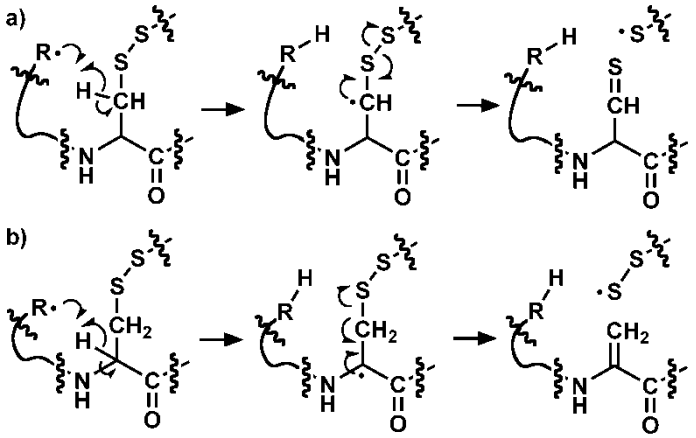

Scheme 2.5 Hydrogen deficient radical disulfide fragmentation. a) Disulfide bond cleavage b) C-S bond dissociation.

2.3.5 Origin of Hydrogen Deficient Radical Chemistry in ECD

The dissociation products observed in ECD from leucine, S-cysteine-acetamide, and disulfide bonds, are consistent with pathways that would be expected from hydrogen deficient radical chemistry. Some of the observed fragmentations do not have plausible hydrogen abundant radical pathways, such as the loss of 56 Da from leucine. It is therefore reasonable to conclude that a significant population of the radicals in charge reduced parent ions of ECD are converted to hydrogen deficient radials. We will now discuss the mechanisms by which hydrogen deficient radicals are created in ECD.

2.3.6 Direct Electron Capture at Charged Sites

NH_3 loss can occur promptly after direct electron capture, and is a commonly observed dissociation in ECD experiments. Loss of NH_3 concomitantly converts the peptide to a hydrogen deficient state, leaving behind a radical at the point of dissociation.[16] It is not surprising, therefore, to note that all of the NH_3 accompanied side chain losses listed in Table 1 are readily explained in terms of hydrogen deficient chemistry. Importantly, NH_3 accompanied side chain losses in ECD experiments represent a substantial fraction of the total listed in Table 2.1; therefore, many of the sidechain losses observed in ECD clearly occur via hydrogen deficient chemistry, but this fact is cloaked by the loss of NH_3 which shifts the masses from the equivalent losses on the right side of Table 2.1.

If direct electron capture occurs on a doubly charged tryptic peptide, the most likely sites for capture are arginine, lysine, and the N-terminus. Direct electron capture at protonated lysine is shown in Scheme 2.6a. A hydrogen abundant radical species is created in the form of a hypervalent $–NH_3$ group. A similar result will be produced by direct electron capture at the N-terminus. In contrast, direct electron capture at a protonated arginine residue, as shown in Scheme 2.6b, yields a hydrogen deficient radical species directly via a loss of a

degree of saturation in the guanidinium moiety. This conversion has been noted previously in quantum mechanical structure calculations.[58] The capacity of arginine to convert directly to a hydrogen deficient radical should lead to observable differences in the dissociation patterns for arginine containing peptides versus lysine containing peptides if there is a competition between hydrogen abundant and hydrogen deficient radical chemistry as postulated herein. The extent to which this difference is observable will also be influenced by the process of H-atom loss.

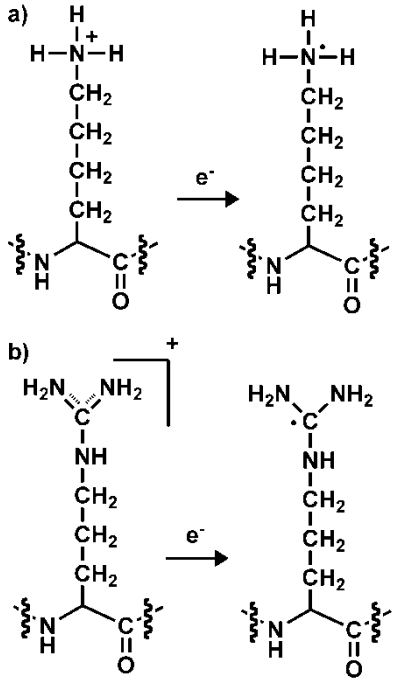

Scheme 2.6 a) Protonated lysine and b) protonated arginine sidechains after direct electron capture at the charge site.

Following direct electron capture, conversion to an even electron species is possible through the loss of an H atom for arginine, lysine and the N-terminus.

The even electron product left behind by H atom loss no longer contains a radical and thus cannot undergo subsequent radical chemistry. Hydrogen atom loss from the charge reduced ion is commonly observed in ECD. One factor that strongly influences H atom loss is peptide size,[1] which is demonstrated in Figure 2.4a. The size effect can be rationalized in a generic fashion by consideration of peptide structure. For doubly charged peptides, shorter sequences will exhibit less intramolecular charge solvation due to increased Coulombic repulsion relative to longer peptides. The results in Figure 2.4a clearly indicate that as charge solvation becomes more favorable in larger peptides, H atom loss is observed less frequently. This further suggests that persistence of the products formed in Scheme 2.6 likely requires significant charge solvation, perhaps to remove energy released from the electron capture event, or to facilitate hydrogen atom transfer.

The pathway shown in Scheme 2.6b implies that arginine may be less susceptible to H atom loss than lysine because arginine can directly access a hydrogen deficient state. Figure 2.4b shows the individual and averaged values of the ratio of charge reduced to H atom loss intensity as a function of peptide size for arginine and lysine containing peptides from the ECD database. Although the predominance of z ions in the database suggests that charge

capture at the N-terminus may occur more commonly than at lysine or arginine, a clear trend is still observed. The results demonstrate that arginine containing peptides are less likely to undergo H atom loss compared to lysine, particularly for larger peptides. As a control, a similar analysis was performed for alanine and glycine which are residues not associated with direct electron capture. No difference is observed between alanine and glycine, as shown in Figure 4c (the statistical sampling breaks down for the largest peptides due to low numbers). These results suggest that the pathway in Scheme 2.6b is one viable route by which electron capture can lead to a hydrogen deficient state.

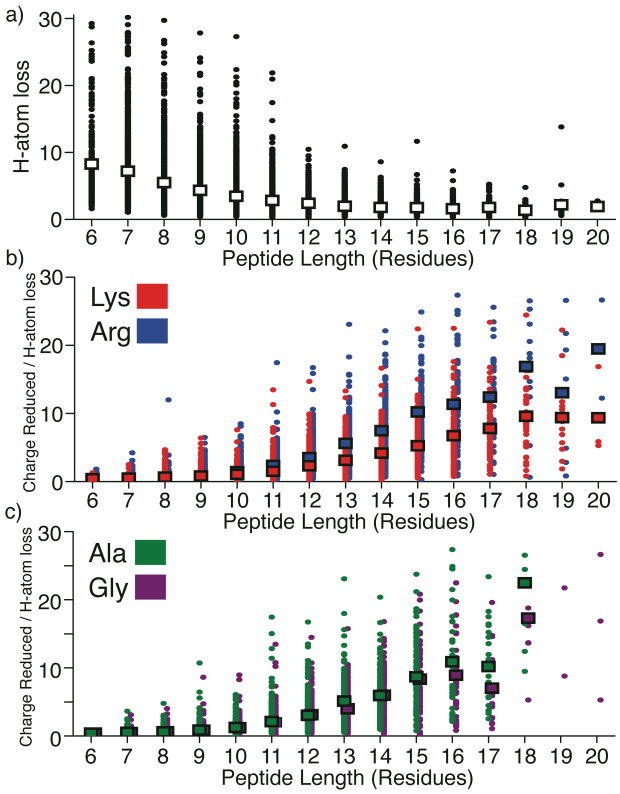

Figure 2.4 (a) Abundance of hydrogen atom sidechain loss as a function of peptide length. The hydrogen atom loss is shown as the fractional abundance relative to the precursor ion. Each peptide is represented as a data point. Histograms for b) arginine or lysine and c) alanine or glycine containing peptides. Ratios of charge reduced parent ion abundance versus hydrogen atom loss after electron capture are plotted as a function of peptide length. In all plots the average values for each peptide length are shown as large squares.

2.3.7 Radical Conversion at the Peptide Backbone

The product generated by direct electron capture at lysine shown in Scheme 2.6a can be converted into a hydrogen deficient radical by several routes. Scheme 2.2c depicts hydrogen atom transfer from a hydrogen abundant moiety to a backbone carbonyl on a peptide. This isobaric conversion from a hydrogen abundant to a hydrogen deficient radical involves loss of a degree of saturation

and forms an aminoketyl radical structure. The aminoketyl radical has been extensively studied by many groups as the proposed immediate precursor to c/z$^{\bullet}$ ion formation; however, the radical structure is hydrogen deficient and is also theoretically capable of hydrogen abstraction. The calculated BDE of the aminoketyl radical structure, 365 kJ/mol, is higher than the average alpha position BDE of ~350 kJ/mol which suggests that radical migration from the aminoketyl to an alpha position would be a reasonable process. Direct synthesis of this radical structure in the gas phase would therefore be extremely useful in answering questions about the propensity of radical migration versus c/z$^{\bullet}$ formation from the aminoketyl radical. Hydrogen deficient radical peptides naturally dissociate via pathways which generate aminoketyl-like radical structures as shown in Scheme 2.7.

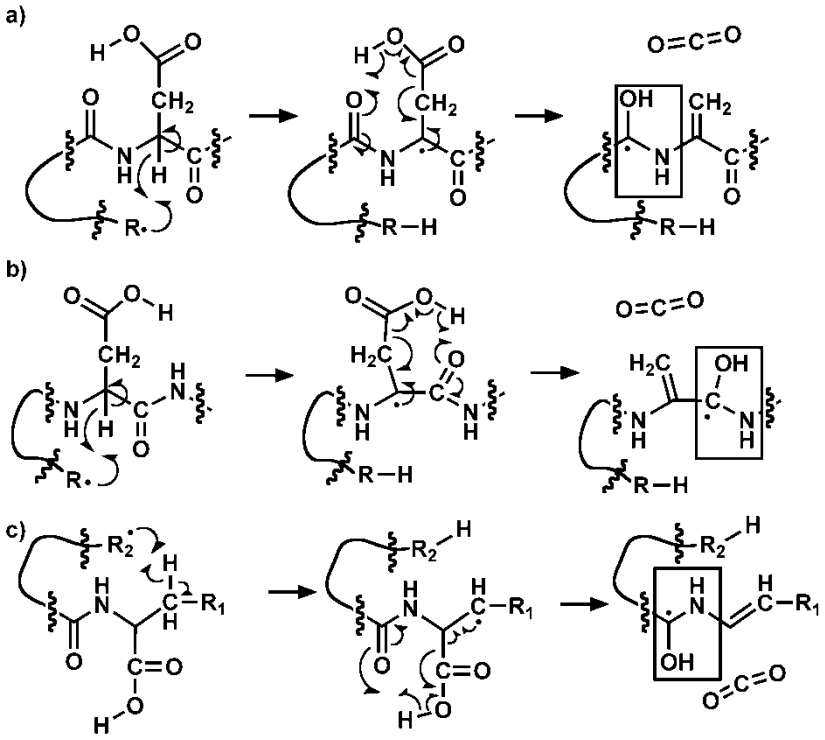

Scheme 2.7 The three pathways which can generate aminoketyl radicals by radical migration; a) aspartic acid pathway I, b) aspartic acid pathway II, c) C-terminal pathway.

Figure 2.4a shows the CID of an aminoketyl radical generated by the C-terminal pathway shown in Scheme 2.7c for the peptide RPPGYSPFR. A significant amount of c_8 ion is formed at the C-terminus in agreement with the anticipated dissociation site for the aminoketyl radical shown in Scheme 2.7c. Hydrogen deficient radical initiated sidechain losses such as 86 Da and 99 Da from arginine are also observed in significant abundance. The fragment ions a_5 and a_8 are also products typical of hydrogen deficient backbone dissociation due to radical migration to the beta positions of aromatic residues in the peptide.[40] Finally the c_5 fragment is related to an aminoketyl mechanism through serine

which does not have an isolatable intermediate.[40] Similar results are obtained with aminoketyl radicals generated in peptides by the mechanisms shown in Scheme 2.7a and 2.7b, although the relative amount of c/z• type dissociation that is observed is reduced. Importantly, c/z• ions are observed adjacent to the expected location of the aminoketyl radical in every case. The relative yields of c/z• ion formation versus hydrogen deficient radical migration observed in Figure 2.5a and similar experiments are not in agreement with results obtained in ECD where the formation of c/z• ions typically dominates.

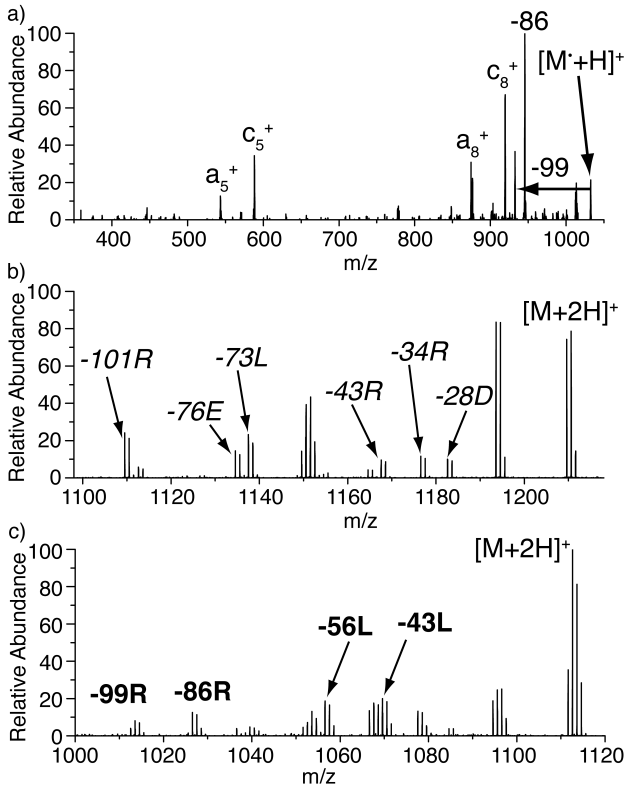

Figure 2.5 a) CID of the aminoketyl radical product from PD/CID of the peptide RPPGY[I]SPFR. b) ECD sidechain loss data for RLEAsLADVR. Hydrogen abundant initiated losses are in italics. c) ECD sidechain loss data for RLEAdLADVR; hydrogen deficient losses are in bold. Lower case 's' represents phosphorylated serine and 'd' represents dehydroalanine.

As stated above, the products in Scheme 2.7 are similar, but not identical to, the aminoketyl radicals generated in ECD. The primary difference relates to the presence of dehydroalanine. As noted previously,[59] dehydroalanine allows delocalization of the radical produced by the pathway in Scheme 2.7b, and interferes with c/z• ion product formation for the aminoketyl radicals generated by the pathways in Scheme 2.7a and 2.7c. Therefore, it is not surprising that modulation of the aminoketyl radical chemistry enables additional hydrogen

deficient radical migration to occur. To confirm the relevance of the results in Figure 2.5a, we conducted further experiments to determine if the presence of dehydroalanine would influence actual ECD experiments. In Figure 2.5b the sidechain loss region of the ECD spectrum for a phosphoserine containing peptide is shown. Typical c/z$^{\bullet}$ fragmentation is observed elsewhere in the spectrum, and most of the side chain losses correspond to hydrogen abundant pathways as can be seen in Table 2.1. Figure 2.5c shows the ECD spectrum for the same peptide where the phosphoserine has been chemically converted to dehydroalanine. Hydrogen deficient sidechain losses from the parent ion such as 99 Da and 86 Da from arginine along with 56 Da and 43 Da from leucine are observed and match by exact mass those given for hydrogen deficient processes in Table 2.1. A significant decrease in c/z$^{\bullet}$ ion formation in the dehydroalanine containing peptide was also observed. These results suggest that modulation of the aminoketyl radical can influence the propensity of this intermediate to undergo c/z$^{\bullet}$ ion formation versus radical migration. It is worth noting that structural effects due to the absence of phosphate may also contribute to the observed differences in dissociation in Figure 2.5. It is likely that peptide sequence, location of charges, hydrogen bonding networks, and other factors influence the microenvironment for each potential aminoketyl radical in a

peptide. Similarly, it is likely that some fraction of these aminoketyl radicals will undergo migration and are therefore a potential source of hydrogen deficient chemistry observed in ECD.

2.3.8 Radical Conversion at Amino Acid Sidechains

Hydrogen atom transfer to the amide sidechains of glutamine and asparagine (as noted previously),[60] and S-cysteine-acetamide produces radical structures similar to the aminoketyl backbone radical shown in Scheme 2.1. Analysis of the fragmentation of these side chains is therefore directly relevant to the backbone dissociation typically observed in ECD. As listed in Table 2.1, analysis of the SwedECD database reveals that 47.1% of Asn containing peptides yield a sidechain loss of 59 Da following hydrogen atom transfer as shown in Scheme 2.8a. This pathway is highly analogous to backbone dissociation which produces c/z$^{\bullet}$ ions. Although a similar mechanism can be drawn for glutamine as shown in Scheme 2.8b, only 5.6% of peptides containing glutamine actually exhibit this loss. The disparity can be rationalized by the stabilities of the nascent radicals. For asparagine, a highly stabilized alpha radical is the product, whereas for glutamine a much less stable primary carbon radical is generated. The calculated transition state energies for the pathways in Scheme 2.8a and 2.8b are also in excellent agreement with the experimental observations. The transition

state energy for asparagine is ~46 kJ/mol, and the loss is somewhat endothermic (ΔH=37 kJ/mol) due to disruption of hydrogen bonding with the side chain. In contrast, the transition state energy for glutamine is ~103 kJ/mol and the reaction is endothermic by 137 kJ/mol. This rationale is further supported by the observation that the same loss of 59 Da from S-cysteine-acetamide occurs with 43.2% regularity and produces a stable sulfur radical[61] as the product. These observations are in excellent agreement with the trends observed for backbone dissociation with the introduction of dehydroalanine into peptides as shown in Figure 2.5 above, i.e. dissociation from an aminoketyl radical can be inhibited by destabilizing the radical product.

A closely related sidechain loss of 60 Da can occur for aspartic and glutamic acid as shown in Scheme 2.9. The relative frequencies are 60.4% and 1.0%, respectively. Again, the results can be rationalized in terms of the stabilities of the radical products.[62] Although sidechain dissociation is disfavored in the cases of Glu and Gln, a stable radical species is formed on the carbonyl carbon that may then undergo hydrogen deficient radical migration. The initially formed sidechain radicals have calculated BDEs of 371 kJ/mol for Glu and 356 kJ/mol for Gln, which are both expected to be able to migrate to lower energy alpha radical positions. These radicals are likely formed on Glu and Gln in high abundance

(based on the amount of dissociation observed for Asp and Asn), and are likely sources of subsequent hydrogen deficient radical chemistry in peptides containing these residues.

Charge remote electron capture at acidic sites (such as the side chains of glutamic and aspartic acid) has not been evaluated previously and may differ substantially from capture at amide sites. It is therefore unknown presently whether charge remote capture analogous to what is predicted at backbone amide sites would be feasible for the side chains of Glu and Asp. Regardless of whether such charge remote capture is subsequently shown to be unlikely, the results can still be rationalized on the basis that Glu and Asp side chains are excellent hydrogen bond partners and are therefore likely to be solvating charges in peptides. This would make them likely targets for H atom attack following electron capture at a protonated site.

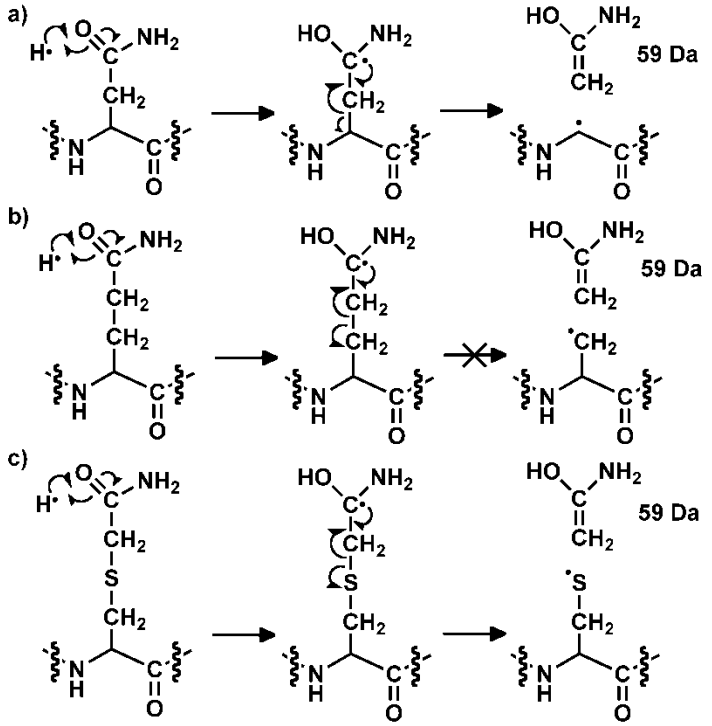

Scheme 2.8 Hydrogen atom attack at a) Asn, b) Gln, and c) S-Cys-acetamide.

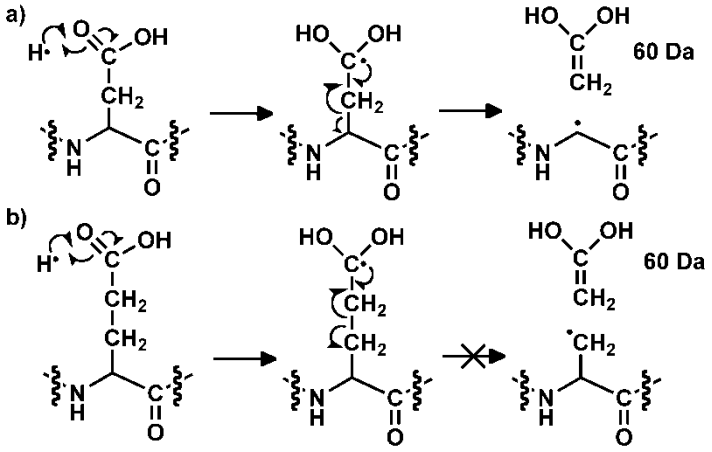

Scheme 2.9 Hydrogen atom attack at a) Asp and b) Glu.

2.4 Conclusions

Many pathways exist for the conversion of hydrogen abundant radicals to hydrogen deficient radicals in ECD. This conversion is key to understanding a

number of sidechain losses which are not readily explained by hydrogen abundant processes alone. Sidechain losses such as -56 Da from leucine and -90 Da from S-cysteine-acetamide in ECD point to both the creation and migration of hydrogen deficient radicals in the charge reduced parent ion. Examination of the SwedECD database also shows that hydrogen deficient sidechain losses are regularly observed after a radical conversion process has taken place, such as the neutral loss of NH_3. The propensity of hydrogen atom loss from the charge reduced parent ion in ECD is directly related to the ability of a hydrogen abundant species to convert to a hydrogen deficient species. As expected, the amount of hydrogen atom loss is therefore dependent on the structure of the charge site as well as the length of the peptide in which it resides. From this information it can be concluded that electron capture can lead directly to a hydrogen deficient species or an initially formed hydrogen abundant radical may quickly convert to a hydrogen deficient radical, which then dictates much of the subsequent observed chemistry that leads to dissociation.

---

[1] Zubarev, R. A.; Kelleher, N. L.; McLafferty, F. W., *J. Am. Chem. Soc.* **1998**, *120*, 3265-3266.

[2] Syka, J. E. P.; Coon, J. J.; Schroeder, M. J.; Shabanowitz, J.; Hunt, D. F., *Proc. Natl. Acad. Sci. USA* **2004**, *101*, 9528-9533.

[3] Zubarev, R. A.; Kruger, N. A.; Fridriksson, E. K.; Lewis, M. A.; Horn, D. M.; Carpenter, B. K.; McLafferty, F. W., *J. Am. Chem. Soc.* **1999**, *121*, 2857-2862.

[4] Guan, Z. Q.; Kelleher, N. L.; OConnor, P. B.; Aaserud, D. J.; Little, D. P.; McLafferty, F. W., *Int. J. Mass Spectrom.* **1996**, *158*, 357-364.
[5] Zubarev, R. A.; Horn, D. M.; Fridriksson, E. K.; Kelleher, N. L.; Kruger, N. A.; Lewis, M. A.; Carpenter, B. K.; McLafferty, F. W., *Anal. Chem.* **2000**, *72*, 563-573.
[6] Kelleher, R. L.; Zubarev, R. A.; Bush, K.; Furie, B.; Furie, B. C.; McLafferty, F. W.; Walsh, C. T., *Anal. Chem.* **1999**, *71*, 4250-4253.
[7] Annan, R. S.; Carr, S. A., *J. Protein Chem.* **1997**, *16*, 391-402.
[8] Zubarev, R., *Expert Review of Proteomics* **2006**, *3*, 251-261.
[9] Swaney, D. L.; McAlister, G. C.; Coon, J. J., *Nat. Methods* **2008**, *5*, 959-964.
[10] Sohn, C. H.; Chung, C. K.; Yin, S.; Ramachandran, P.; Loo, J. A.; Beauchamp, J. L., *J. Am. Chem. Soc.* **2009**, *131*, 5444-5459.
[11] Anusiewicz, W.; Berdys-Kochanska, J.; Simons, J., *J. Phys. Chem. A* **2005**, *109*, 5801-5813.
[12] Breuker, K.; Oh, H. B.; Lin, C.; Carpenter, B. K.; McLafferty, F. W., *Proc. Natl. Acad. Sci. USA* **2004**, *101*, 14011-14016.
[13] Turecek, F., *J. Am. Chem. Soc.* **2003**, *125*, 5954-5963.
[14] Zubarev, R. A.; Haselmann, K. F.; Budnik, B.; Kjeldsen, F.; Jensen, F., *Eur. J. Mass Spectrom.* **2002**, *8*, 337-349.
[15] Savitski, M. M.; Nielsen, M. L.; Zubarev, R. A., *Anal. Chem.* **2007**, *79*, 2296-2302.
[16] Falth, M.; Savitski, M. M.; Nielsen, M. L.; Kjeldsen, F.; Andren, P. E.; Zubarev, R. A., *Anal. Chem.* **2008**, *80*, 8089-8094.
[17] Cooper, H. J.; Hudgins, R. R.; Hakansson, K.; Marshall, A. G., *J. Am. Soc. Mass. Spectrom.* **2002**, *13*, 241-249.
[18] Laskin, J.; Yang, Z. B.; Lam, C.; Chu, I. K., *Anal. Chem.* **2007**, *79*, 6607-6614.
[19] Leymarie, N.; Costello, C. E.; O'Connor, P. B., *J. Am. Chem. Soc.* **2003**, *125*, 8949-8958.
[20] Li, X. J.; Cournoyer, J. J.; Lin, C.; O'Connor, P. B., *J. Am. Soc. Mass. Spectrom.* **2008**, *19*, 1514-1526.
[21] Chung, T. W.; Turecek, F., *J. Am. Soc. Mass Spectrom.* **2010,** *21* (8), 1279-1295.
[22] Ly, T.; Julian, R. R., *J. Am. Chem. Soc.* **2008**, *130*, 351-358.
[23] Diedrich, J. K.; Julian, R. R., *Anal. Chem.* **2010,** *82*, 4006-4014.
[24] Reed, D. R.; Hare, M.; Kass, S. R., *J. Am. Chem. Soc.* **2000**, *122*, 10689-10696.
[25] Budnik, B. A.; Haselmann, K. F.; Zubarev, R. A., *Chem. Phys. Lett.* **2001**, *342*, 299-302.
[26] Anusiewicz, I.; Jasionowski, M.; Skurski, P.; Simons, J., *J. Phys. Chem. A* **2005,** *109*, 11332-11337.
[27] Ly, T.; Yin, S.; Loo, J. A.; Julian, R. R., *Rapid Commun. Mass Spectrom.* **2009**, *23*, 2099-2101.
[28] Hao, G.; Gross, S. S., *J. Am. Soc. Mass. Spectrom.* **2006**, *17*, 1725-1730.
[29] Masterson, D. S.; Yin, H. Y.; Chacon, A.; Hachey, D. L.; Norris, J. L.; Porter, N. A., *J. Am. Chem. Soc.* **2004**, *126*, 720-721.
[30] Hodyss, R.; Cox, H. A.; Beauchamp, J. L., *J. Am. Chem. Soc.* **2005**, *127*, 12436-12437.

[31] Chu, I. K.; Rodriguez, C. F.; Rodriguez, F.; Hopkinson, A. C.; Siu, K. W. M., *J. Am. Soc. Mass. Spectrom.* **2001**, *12*, 1114-1119.
[32] Barlow, C. K.; Moran, D.; Radom, L.; McFadyen, W. D.; O'Hair, R. A. J., *J. Phys. Chem. A* **2006**, *110*, 8304-8315.
[33] Kalcic, C. L.; Gunaratne, T. C.; Jonest, A. D.; Dantus, M.; Reid, G. E., *J. Am. Chem. Soc.* **2009**, *131*, 940-942.
[34] O'Connor, P. B.; Lin, C.; Cournoyer, J. J.; Pittman, J. L.; Belyayev, M.; Budnik, B. A., *J. Am. Soc. Mass. Spectrom.* **2006**, *17*, 576-585.
[35] Han, H. L.; Xia, Y.; McLuckey, S. A., *Journal of Proteome Research* **2007**, *6*, 3062-3069.
[36] Chung, T. W.; Turecek, F., *J. Am. Soc. Mass. Spectrom.* **2010**, *21*, 1279-1295.
[37] Tsybin, Y. O.; He, H.; Emmett, M. R.; Hendrickson, C. L.; Marshall, A. G., *Anal. Chem.* **2007,** *79*, 7596-7602.
[38] Ben Hamidane, H.; Chiappe, D.; Hartmer, R.; Vorobyev, A.; Moniatte, M.; Tsybin, Y. O., *J. Am. Soc. Mass. Spectrom.* **2009,** *20*, 567-575.
[39] Savitski, M. M.; Kjeldsen, F.; Nielsen, M. L.; Zubarev, R. A., *J. Am. Soc. Mass. Spectrom.* **2007,** *18*, 113-120.
[40] Sun, Q. Y.; Nelson, H.; Ly, T.; Stoltz, B. M.; Julian, R. R., *Journal of Proteome Research* **2009**, *8*, 958-966.
[41] Moore, B. N.; Blanksby, S. J.; Julian, R. R., *Chem. Commun.* **2009,** (33), 5015-5017.
[42] Ly, T.; Julian, R. R., *J. Am. Soc. Mass Spectrom.* **2009,** *20*, 1148-1158.
[43] Turecek, F.; Syrstad, E. A., *J. Am. Chem. Soc.* **2003**, *125*, 3353-3369.
[44] Ly, T.; Julian, R. R., *J. Am. Chem. Soc.* **2010**, *132*, 8602-8609.
[45] Syrstad, E. A.; Turecek, F., *J. Am. Soc. Mass. Spectrom.* **2005**, *16*, 208-224.
[46] Sobczyk, M.; Anusiewicz, W.; Berdys-Kochanska, J.; Sawicka, A.; Skurski, P.; Simons, J., *J. Phys. Chem. A* **2005**, *109*, 250-258.
[47] Regoeczi, E., *Iodine-labeled Plasma Proteins*. CRC Press: Boca Raton, FL, 1984.
[48] Chan, W. C.; White, P. D., *Fmoc Solid Phase Peptide Synthesis: A Practical Approach.* Oxford University Press: New York, NY, 2004.
[49] Sechi, S.; Chait, B. T., *Anal. Chem.* **1998,** *70*, 5150-5158.
[50] Klemm, C.; Schroder, S.; Gluckmann, M.; Beyermann, M.; Krause, E., *Rapid Commun. Mass Spectrom.* **2004,** *18*, 2697-2705.
[51] Tam, J. P.; Wu, C. R.; Liu, W.; Zhang, J. W., *J. Am. Chem. Soc.* **1991,** *113*, 6657-6662.
[52] Frisch, M. J.; et al. *Gaussian 03, Revision D.01*, Gaussian, Inc.: Wallingford CT, 2004.
[53] Rauk, A.; Yu, D.; Taylor, J.; Shustov, G. V.; Block, D. A.; Armstrong, D. A., *Biochemistry* **1999**, *38*, 9089-9096.
[54] Peng, C. Y.; Schlegel, H. B., *Isr. J. Chem.* **1993,** *33*, 449-454.
[55] Viehe, H. G.; Janousek, Z.; Merenyi, R.; Stella, L., *Acc. Chem. Res.* **1985**, *18*, 148-154.
[56] Hopkinson, A. C., *Mass Spectrom. Rev.* **2009**, *28*, 655-671.
[57] Sohn, C. H.; Kim, T.-Y.; Beauchamp, J. L., Fundamental Studies of Inter- and Intramolecular Disulfide Bond Cleavages in Model Peptides by Covalently Attached

Acetyl Radical *Conference on Ion Chemistry and Mass Spectrometry*, Lake Arrowhead, CA, Jan 14-16, 2011.

[58] Panja, S.; Nielsen, S. B.; Hvelplund, P.; Turecek, F., *J. Am. Soc. Mass. Spectrom.* **2008**, *19*, 1726-1742.

[59] Chung, T. W.; Turecek, F., *Int. J. Mass Spectrom.* **2011,** *301* (1-3), 55-61.

[60] Haselmann, K. F.; Budnik, B. A.; Kjeldsen, F.; Polfer, N. C.; Zubarev, R. A., *Eur. J. Mass Spectrom.* **2002,** *8*, 461-469.

[61] Rauk, A.; Yu, D.; Armstrong, D. A., *J. Am. Chem. Soc.* **1998**, *120*, 8848-8855.

[62] Li, X. J.; Lin, C.; O'Connor, P. B. *Anal. Chem.* **2010**, *82*, 3606.

Chapter 3

Dissociation Energies of X-H Bonds in Amino Acids

3.1 Introduction

Radical chemistry in biological systems is an important area of interest and has been studied extensively.[1,2] Living organisms require free radical chemistry to perform certain tasks and thus radicals are necessary for survival.[3,4] For instance, the enzyme ribonucleotide reductase utilizes radical chemistry to catalyze the conversion of ribonucleotides to deoxyribonucleotides, an essential process for the replication of DNA.[5] In contrast, the protein complex myeloperoxidase utilizes radical chemistry to generate reactive oxygen species that are used by neutrophils to indiscriminately destroy bacteria.[6] These juxtaposing utilities make it easy to see that radicals are both useful and also potentially dangerous in living organisms. In fact, many biomolecules including nucleic acids, proteins, and lipids are irreversibly modified or destroyed upon exposure to free radical species, which are abundantly present in biological systems.[1]

Although radical chemistry is frequently complex, the focus presently will be on hydrogen abstraction reactions, as in the example shown in Scheme 3.1.

Hydrogen abstraction is always accompanied by radical migration because as the hydrogen is transferred from one atom to another, a radical is created in the newly unoccupied position. Hydrogen abstraction can occur intramolecularly or intermolecularly. Repeated hydrogen abstraction can lead to significant migration of the radical away from the site where it was initially formed. In the context of protein chemistry, this is important because damage may occur both at the initial, intermediate, and final locations of the radical through a variety of different mechanisms. To cite one interesting example, abstraction of hydrogen from a chiral center can lead to racemization when the radical is quenched by further hydrogen abstraction.[7] Such modifications are very difficult to detect, hence a detailed understanding of radical migration in proteins is important. Radical migration is mediated by both kinetic and thermodynamic constraints. The kinetics are largely determined by structural parameters, which vary greatly from molecule to molecule and will not be emphasized herein. The thermodynamics of radical migration can be accurately approximated with knowledge of the bond dissociation energies (BDEs) for each X-H bond (where X=C, N, S, O) that can potentially undergo hydrogen abstraction. For example, the energetic feasibility of abstraction of hydrogen from the side chain of alanine by •OH can be fairly reasonably estimated by knowledge of the H-OH and H-

CH_2CH_3 BDEs, which are 494 and 423 kJ/mol, respectively. Abstraction of hydrogen in this example would be predicted to be exothermic by ~71kJ/mol. This estimation ignores the influence that other local structural factors may have on the BDE, which can be significant in some cases as described in further detail below.

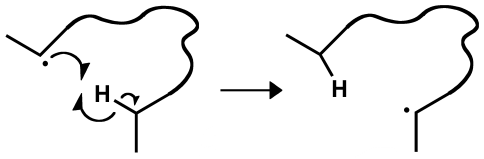

Scheme 3.1 Generic radical transfer mechanism via hydrogen atom abstraction.

BDEs are also useful in the prediction of dissociation pathways. Scheme 3.2 shows a hypothetical radical rearrangement which could follow one of two pathways. Assuming the X• has a lower BDE than both A• and B•, the rearrangement leading to formation of a double bond by either mechanism will be endothermic. If the A• product has a lower BDE than the B• product, formation of the A• product will likely be favored and *vice versa*. The ratio of products A• and B• therefore depends strongly on the BDE of A• and B•.

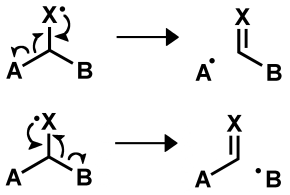

Scheme 3.2 Model of competing radical dissociation pathways. The initiating radical starts on the X atom and is capable of rearranging via beta cleavage to form either A radical or B radical.

BDEs for many chemical systems have been determined in the past by both experiment and theory.[8] Experimental methods include halogen radical hydrogen abstraction kinetic studies, gas-phase acidity cycles, photoionization mass spectrometry[9], and photoacoustic calorimetry.[10] All of these experiments can be difficult to perform and are only suitable for simple and relatively small molecules. Scheme 3.3 contains the experimentally derived BDEs for a few molecules which contain chemical structures reminiscent of the functional groups typically found in a protein. Experimentally derived BDEs for larger molecules are not realistically possible.

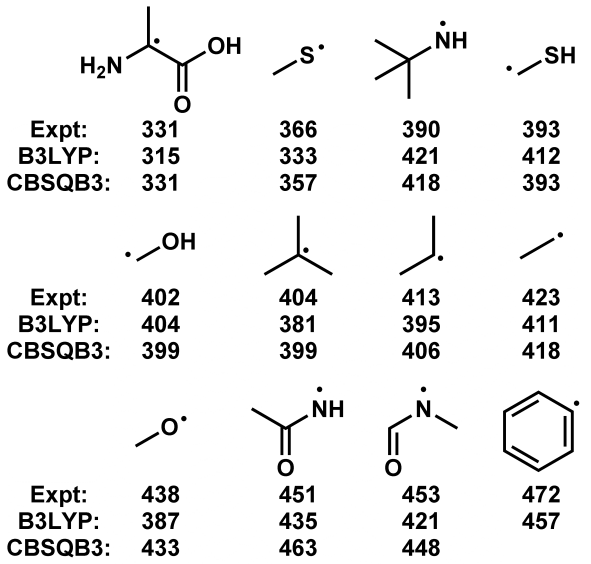

Scheme 3.3 Experimentally determined and theoretically calculated BDEs of simple molecules with chemical structures similar to those found in the amino acid sidechains, peptide termini, and backbone. Bond dissociation energies are in kJ/mol. Theoretical BDEs were calculated directly by the CBSQB3 method and by the B3LYP/6-31G(d) method.

Theory is amenable to larger systems that are inaccessible by direct experiment. Accurate BDE values can be obtained by *ab initio* quantum mechanical calculations when appropriate methods are used. Caution is recommended with *de novo* calculations at low levels of theory, which do not take into account any experimental results, as they can be inaccurate even for small molecules. Scheme 3.3 gives a comparison of this for a variety of molecules with chemical structures typically found in peptides. The BDE of a C-H bond in CH_3SH as calculated by direct hydrogen atom abstraction at the B3LYP/6-31G(d) level of theory is 412 kJ/mol while the experimentally determined BDE is 393±8

kJ/mol. Higher levels of theory and larger basis sets can remedy this problem, but only at the cost of additional computational time and resources (which can become excessive for larger molecules). A complete basis set extrapolation calculation (CBSQB3)[11] of the CH_3SH BDE mentioned above gives a BDE of 393 kJ/mol which is identical to the experimental value, but also required a 6-fold increase in computation time. As an alternative to computationally intensive methods, the error resulting from less expensive calculations can be drastically minimized through the use of isodesmic reactions. An isodesmic reaction is one in which the locations of bonds are changed while the types of bonds are unaltered. An experimentally determined BDE is used as a reference to cancel out systematic error in calculated energies. This technique can be used to calculate the BDE of any radical center of interest given that a structurally similar radical has been previously probed experimentally. This method has been used to successfully calculate BDEs for amino acids and other biomolecules in the past. Rauk and coworkers have previously calculated BDEs for alpha carbon radicals[12] and all radicals on cysteine[13], alanine, serine, and threonine.[14] Julian and coworkers have previously calculated BDEs for β radicals.[15] Kar and coworkers have previously calculated BDEs for leucine.[16] These energies have been recalculated in this work according to the criteria mentioned above to

present a level comparison among all of the amino acids. In general, the BDEs presented here are in good agreement with those found in the literature.

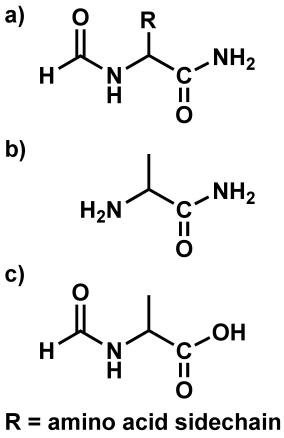

Scheme 3.4 Calculation models for a) an amino acid in an extended sequence, b) the N-terminus, and c) the C-terminus.

Herein, the BDEs for all X-H bonds present in the sidechains, backbone, N- and C- termini of proteins are calculated. The twenty canonical amino acids are all considered, in both charged and neutral states (when appropriate). The range of BDEs scales from 319 kJ/mol to 527 kJ/mol. The alpha carbon functional groups have the lowest BDEs, due to the captodative effect. Tertiary and secondary carbon centers are of intermediate stability. The primary and aromatic carbons have the highest BDEs. These results are consistent with previous understanding of radical chemistry and follow the general trend of carbocation stability. Although these trends are generally true, specific exceptions have been observed and are examined in detail.

3.2 Experimental Details

Calculations were performed using Gaussian 09 Rev. A.1 (Gaussian, Inc., Wallingford, CT).[17] Structural optimizations and energy calculations were done with hybrid density functional theory B3LYP at the 6-31G(d) basis set unless otherwise stated. All BDEs were calculated by the isodesmic reaction method[18] using experimentally determined BDEs of suitable reference molecules.[8,19,20] For example, if the BDE of the O-H bond in ethanol, CH_3CH_2OH, was of interest and had not been previously determined, the experimentally derived BDE of the very similar O-H bond found in methanol, CH_3OH, could be used to determine ethanol's O-H BDE via the isodesmic reaction method. An isodesmic reaction in which bond types are preserved could be setup as follows: $CH_3CH_2OH + CH_3O\bullet \rightarrow CH_3CH_2O\bullet + CH_3OH$. Quantum mechanical calculation of the energies of each of these species would then yield a ΔH of reaction. Setting this ΔH equal to the experimental equivalent of the isodesmic reaction gives $\Delta H_{calculated}$ = BDE(ethanol) – BDE(methanol) where BDE(methanol) is given by experiment and BDE(ethanol) is the quantity to be solved for. In this work, hypothetical hydrogen atom abstractions were created between the molecule of interest (an amino acid with a single hydrogen removed) and a reference molecule. Reference molecules were chosen such that the X-H bond being broken in the

reference system was as similar as possible to the X-H bond being examined in the BDE calculation. Since the same bonds are present in the products and reactants, systematic error in the calculation of the absolute energies of each molecule should cancel. The experimental BDE of the reference system was then used to offset the calculated values and a BDE for the molecule of interest was extracted. The absolute error for BDEs calculated by this method and level of theory are approximately ±10 kJ/mol.

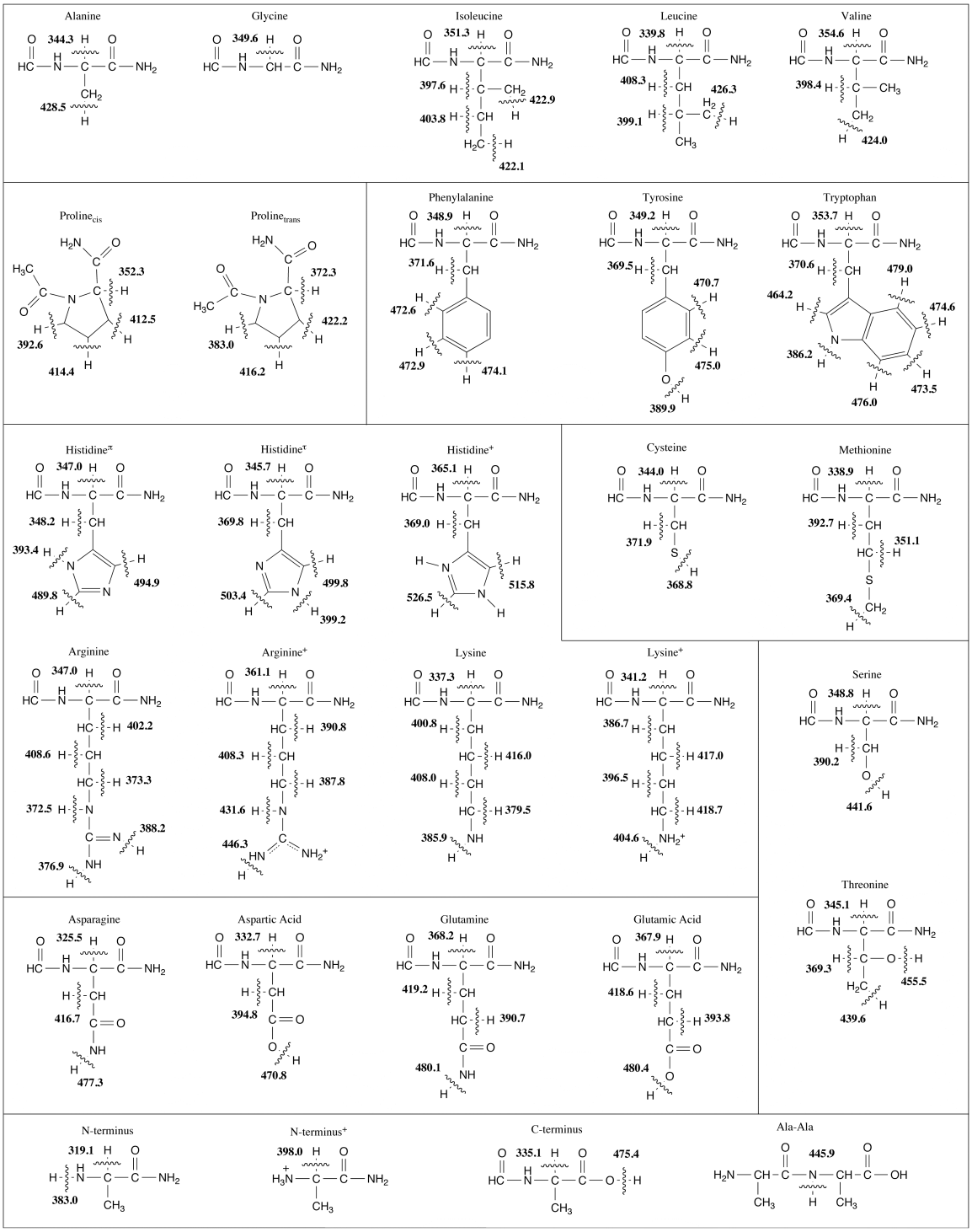

Chart 3.1 BDEs of X-H bonds in all 20 proteinogenic amino acids, peptide backbone, and termini.

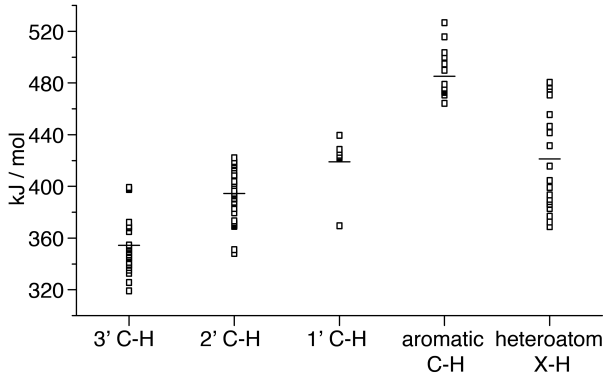

Figure 3.1 BDEs of all X-H bonds in the amino acids and termini grouped by chemical structure. In each category empty squares denote BDE values of specific X-H bonds. A horizontal bar represents the average BDE of each category.

Amino acids were modeled as being part of a typical peptide backbone by extending the N-terminus by a formyl group and by converting the C-terminus into an amide as shown in Scheme 3.4a. Proline was extended on the N-terminus by an acetyl group, an additional methyl compared to Scheme 4a, in order to better model the effects of the cis and trans conformational states. Extended versions of alanine were used as models for the N-terminus and C-terminus as shown in Scheme 3.4b and 3.4c respectively. For each amino acid, conformational minima were chosen that eliminated energetic artifacts due to changes in sidechain-backbone interactions when comparing radical and nonradical structures. In this way most of the calculated BDE directly results from the elimination of the hydrogen atom. Although structural rearrangement as a result of hydrogen atom transfer will affect actual BDEs in peptide and protein

systems, these effects are dependent on the peptide sequence and local environment of the amino acid and are not considered in this study.

3.3 Results and Discussion

Bond dissociation energies of 114 X-H bonds present in the 20 proteinogenic amino acids were calculated by the isodesmic reaction method. Chart 3.1 presents this complete set of BDE values including those of the basic amino acids and N-terminus in their neutral and protonated forms. The tautomers of histidine, cis and trans conformations of proline, and the protein termini and backbone were also included in the analysis. The amino acids in Chart 3.1 are organized by sidechain chemical structure.

In order to predict sites of favored radical attack and subsequent pathways of radical migration it is useful to group BDEs according to chemical and energetic similarities. Figure 3.1 shows the BDEs of all of the examined bonds grouped into 5 categories by chemical structure. Tertiary carbon radicals are most stable followed by secondary and primary carbon radicals. Aromatic carbon radicals are the least stable while heteroatom radicals span a significant portion of the BDE range. The BDEs follow the trends anticipated given their chemical structure, with the exception of a few outliers which will be examined in more detail.

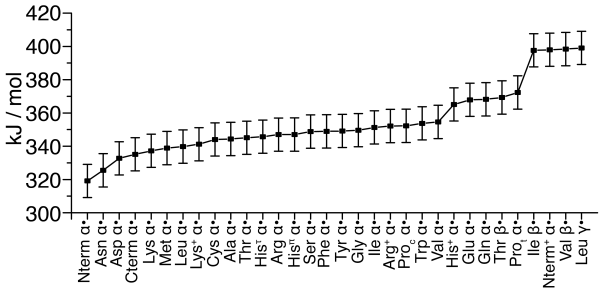

Figure 3.2 Tertiary C-H BDEs in the amino acids and termini.

3.3.1 Tertiary Carbon Radical Centers

Figure 3.2 shows the BDE values corresponding to all tertiary carbon radicals present in amino acids which range from 319 kJ/mol to 399 kJ/mol. Tertiary carbon radicals are generally among the more stable species that can be present in proteins. Most of the tertiary carbon atoms are α carbons, which are particularly stable due to the captodative effect.[21] These radicals have been the subject of extensive theoretical study due to their stability and abundance in proteins. The effect of captodative stabilization is clearly shown in Figure 3.2 where the α radicals are consistently more stable than other tertiary carbons. An exception to this is the α radical on the protonated N-terminus. In captodative stabilization, the N-terminal side of the α carbon is electron-donating while the C-terminal carbon is electron-withdrawing. In this work the N-terminus has been modelled as an N-terminal alanine residue as shown in Scheme 3.4b. Laskin and coworkers have previously shown that the captodative effect is enhanced for

neutral N-terminal amino acids, which are terminated by an amine rather than an amide.[22] This increased stability can be seen in Figure 3.2 by comparison of Ala $\alpha\bullet$ to Nterm $\alpha\bullet$ where the latter is more stable by 16 kJ/mol. However, when the N-terminus is protonated, $Nterm^{+}$ $\alpha\bullet$ in Figure 3.2, the electron-donating ability of the N-terminus is reduced thus disrupting the captodative effect and decreasing the stability of the α carbon radical by 79 kJ/mol. A similar destabilization effect will likely occur for an α carbon next to a deprotonated C-terminus.

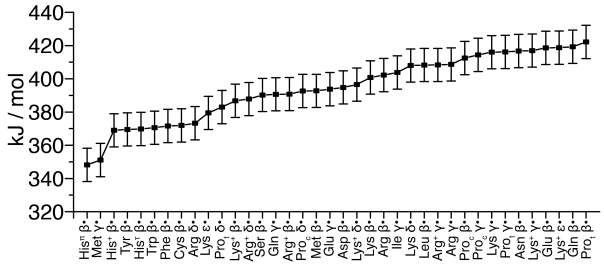

Figure 3.3 Secondary C-H BDEs in amino acids.

3.3.2 Secondary Carbon Radical Centers.

Figure 3.3 shows the BDE values of all secondary carbon radicals in the amino acids, which span from 348 kJ/mol to 419 kJ/mol. The β carbons on aromatic amino acids (His, Tyr, Trp, and Phe) do not exceed 372 kJ/mol and are significantly more stable than the other secondary carbons. This stability has been previously observed and plays an important role in the gas phase radical dissociation of peptide and proteins.[23] Beta cleavage from these radicals yields

distinct backbone dissociation, which has been observed in gas-phase radical peptide experiments.[24]

As seen in Figure 3.3, the γ position of methionine (351 kJ/mol) and the β position of cysteine (372 kJ/mol) are both significantly stabilized by their proximity to a sulfur atom. The stability of radicals on these sulfur-containing residues has been previously noted and has been linked to their presence in active sites of radical utilizing proteins.[13] A radical at the β position of cysteine is capable of undergoing beta cleavage backbone dissociation while the radical at the γ position of methionine has a dissociative pathway yielding $CH_2CH_2SCH_3$ and a glycine α radical.[15]

The second lowest BDE in Figure 3.3 is that of the β position of His^{π}. His^{π} and His^{τ} are the two tautomers of histidine as shown in Chart 3.1. The β position of His^{π} is 22 kJ/mol more stable than the β position of His^{τ} and 21 kJ/mol more stable than the β position of protonated histidine, His^{+}. This increase in stability may be attributed to the ability of His^{π} to delocalize the β radical into the aromatic sidechain. Tautomerization of histidine occurs through protonation and deprotonation at the τ and π nitrogens and at pH 7 the amino acid of histidine is expected to be approximately 20% His^{π} and 80% His^{τ}.[25,26] Although the exchange between His^{π} and His^{τ} is a solution phase process requiring protonation, it is

worthwhile to note that in the gas phase tautomer His^{τ} is slightly more favorable than His^{π} by 5.8 kJ/mol.

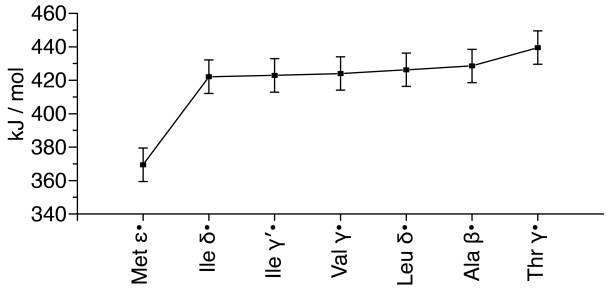

Figure 3.4 Primary C-H BDEs in amino acids.

3.3.3 Primary Carbon Radical Centers

Figure 3.4 shows the BDE values of all primary carbon radicals in the amino acids. Most of the primary carbon BDEs fall within the 420 kJ/mol to 450 kJ/mol range. Radicals located at primary carbons are expected to be very unstable. This assumption is true with the exception of the primary carbon of methionine. The ε position of methionine has a BDE of 369 kJ/mol which is in the range of the secondary carbon BDEs. Again, proximity to the sulfur atom contributes to the stability of a radical at this position. The dissociative pathway from the methionine ε radical would yield an energetically unstable primary carbon centered radical and is not likely to occur. These radicals also have fairly unfavorable dissociation pathways, the exception being the β position of alanine

which has a facile backbone dissociation pathway which has been observed previously.[27]

3.3.4 Aromatic Carbon Radical Centers

Figure 3.5 shows the BDEs of all aromatic carbon radicals in the amino acids. These positions have the highest BDEs in peptides and proteins and are the least stable radical centers. All of these energies are above 460 kJ/mol making them very unstable relative to the other C-H BDEs previously mentioned.

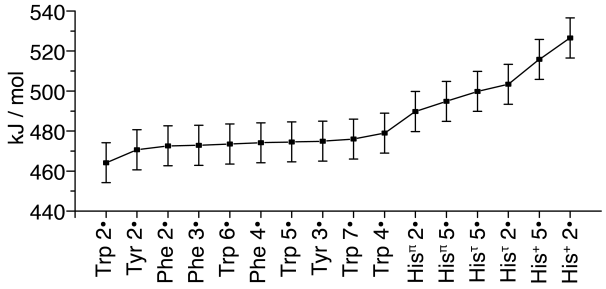

Figure 3.5 Aromatic C-H BDEs in amino acids.

The highest BDE in this work is that of the 2 position of protonated histidine at 527 kJ/mol. The aromatic radicals do not have directly accessible favorable dissociative pathways and are not expected to be stable radical migration sites due to their high energetic instability. These radicals may be accessible in systems where the initiating radical is extremely unstable such as OH• (497 kJ/mol).[8] It has been observed that radical migration will quickly transfer aromatic radicals to other kinetically available sites.[28,29]

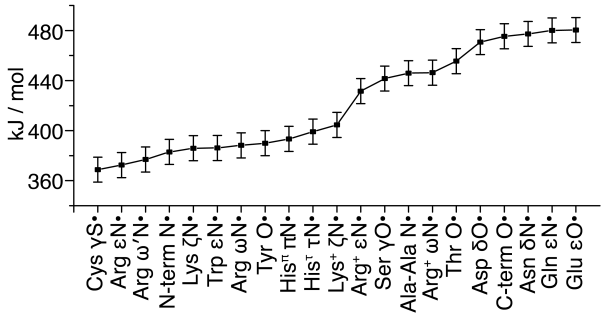

Figure 3.6 Heteroatom X-H BDEs in the amino acids, termini, and peptide backbone.

3.3.5 Heteroatom Radical Centers

Finally we consider heteroatoms as radical centers. Figure 3.6 shows the BDEs of all heteroatom radicals in the amino acids and termini. The BDEs of heteroatom radicals range from 369 kJ/mol to 480 kJ/mol and overlap with the secondary, primary, and aromatic C-H BDEs. Cysteine S-H has the lowest heteroatom BDE at 369 kJ/mol, similar to that of glutathione (367 kJ/mol)[13], and is in the range of secondary carbons while the carboxylic acid O-H of glutamic acid has the highest BDE at 480 kJ/mol, in the range of the aromatic carbon BDEs. Amide N-H BDEs on the peptide backbone were modeled in the dipeptide Ala-Ala. The backbone amide N-H BDE is also relatively high at 446 kJ/mol. Peptide backbone amides as well as sidechain amides are not likely destinations of radical migration due to the abundance of other available sites of higher stability. Aromatic heteroatoms, primary amines and the sulfur of cysteine are the most

likely heteroatoms to host a radical. The sulfur radical of cysteine has a favorable dissociative pathway via the loss of CH_2S. Heteroatom radicals on serine, threonine, and tyrosine also have favorable fragmentation routes.

3.4 Conclusion

Radical chemistry affords biological systems the unique ability to easily create and destroy chemical bonds between many types of chemical functionalities. This power is harnessed by proteins through the use of complex energetic and kinetic landscapes, which direct radicals to active sites or to other areas of the cell. Although radicals are generally thought of as destructive tools, they are not indiscriminate and will follow general trends that will dictate where they are most likely to attack. Knowledge of the factors that control radical stability and radical migration is essential to understanding protein radical chemistry. The X-H BDEs in the 20 proteinogenic amino acids offer at least the primary information needed to predict the behavior of radicals in proteins while kinetics and fragmentation thermodynamics provide the complete picture.

---

[1] Halliwell, B.; Gutteridge, J. M. C., Free Radicals in Biology and Medicine. 4th ed. Oxford, NY: Oxford University Press; 2007.

[2] Droge, W., Free radicals in the physiological control of cell function. Physiol. Rev. 82: 47-95; 2002.

[3] Stubbe, J.; van der Donk, W. A., Protein radicals in enzyme catalysis. Chem. Rev. 98: 705-762; 1998.

[4] Valko, M.; Leibfritz, D.; Moncol, J.; Cronin, M. T. D.; Mazur, M.; Telser, J., Free radicals and antioxidants in normal physiological functions and human disease. Int. J. Biochem. Cell Biol. 39: 44-84; 2007.

[5] Nordlund, P.; Sjoberg, B. M.; Eklund, H., 3-Dimensional Structure of the Free-Radical Protein of Ribonucleotide Reductase. Nature 345: 593-598; 1990.

[6] Klebanoff, S. J., Myeloperoxidase: friend and foe. J. Leukocyte Biol. 77: 598-625; 2005.

[7] Lubec, G.; Weninger, M.; Anderson, S. R., Racemization and Oxidation Studies of Hair Protein in the Homo-Tirolensis. FASEB J. 8: 1166-1169; 1994.

[8] Blanksby, S. J.; Ellison, G. B., Bond dissociation energies of organic molecules. Acc. Chem. Res. 36: 255-263; 2003.

[9] Berkowitz, J.; Ellison, G. B.; Gutman, D., 3 Methods to Measure Rh Bond-Energies. J. Phys. Chem. 98: 2744-2765; 1994.

[10] Laarhoven, L. J. J.; Mulder, P.; Wayner, D. D. M., Determination of bond dissociation enthalpies in solution by photoacoustic calorimetry. Acc. Chem. Res. 32: 342-349; 1999.

[11] Montgomery, J. A.; Frisch, M. J.; Ochterski, J. W.; Petersson, G. A., A complete basis set model chemistry. VI. Use of density functional geometries and frequencies. J. Chem. Phys. 110: 2822-2827; 1999.

[12] Rauk, A.; Yu, D.; Taylor, J.; Shustov, G. V.; Block, D. A.; Armstrong, D. A., Effects of structure on C-alpha-H bond enthalpies of amino acid residues: Relevance to H transfers in enzyme mechanisms and in protein oxidation. Biochemistry 38: 9089-9096; 1999.

[13] Rauk, A.; Yu, D.; Armstrong, D. A., Oxidative damage to and by cysteine in proteins: An ab initio study of the radical structures, C-H, S-H, and C-C bond dissociation energies, and transition structures for H abstraction by thiyl radicals. J. Am. Chem. Soc. 120: 8848-8855; 1998.

[14] Rauk, A.; Yu, D.; Armstrong, D. A., Toward site specificity of oxidative damage in proteins: C-H and C-C bond dissociation energies and reduction potentials of the radicals of alanine, serine, and threonine residues - An ab initio study. J. Am. Chem. Soc. 119: 208-217; 1997.

[15] Sun, Q. Y.; Nelson, H.; Ly, T.; Stoltz, B. M.; Julian, R. R., Side Chain Chemistry Mediates Backbone Fragmentation in Hydrogen Deficient Peptide Radicals. J. Proteome Res. 8: 958-966; 2009.

[16] Scheiner, S.; Kar, T., Analysis of the Reactivities of Protein C-H Bonds to H Atom Abstraction by OH Radical. J. Am. Chem. Soc. 132: 16450-16459; 2010.

[17] Frisch, M. J.; Trucks, G. W.; Schlegel, H. B.; Scuseria, G. E.; Robb, M. A.; Cheeseman, J. R.; Scalmani, G.; Barone, V.; Mennucci, B.; Petersson, G. A.; Nakatsuji, H.; Caricato, M.; Li, X.; Hratchian, H. P.; Izmaylov, A. F.; Bloino, J.; Zheng, G.; Sonnenberg, J. L.; Hada, M.; Ehara, M.; Toyota, K.; Fukuda, R.; Hasegawa, J.; Ishida, M.; Nakajima, T.; Honda, Y.; Kitao, O.; Nakai, H.; Vreven, T.; J. A. Montgomery, J.; Peralta, J. E.;

Ogliaro, F.; Bearpark, M.; Heyd, J. J.; Brothers, E.; Kudin, K. N.; Staroverov, V. N.; Kobayashi, R.; Normand, J.; Raghavachari, K.; Rendell, A.; Burant, J. C.; Iyengar, S. S.; Tomasi, J.; Cossi, M.; Rega, N.; Millam, J. M.; Klene, M.; Knox, J. E.; Cross, J. B.; Bakken, V.; Adamo, C.; Jaramillo, J.; Gomperts, R.; Stratmann, R. E.; Yazyev, O.; Austin, A. J.; Cammi, R.; Pomelli, C.; Ochterski, J. W.; Martin, R. L.; Morokuma, K.; Zakrzewski, V. G.; Voth, G. A.; Salvador, P.; Dannenberg, J. J.; Dapprich, S.; Daniels, A. D.; Farkas, Ö.; Foresman, J. B.; Ortiz, J. V.; Cioslowski, J.; Fox, D. J. Gaussian 09, Revision A.1; Gaussian, Inc.: Wallingford CT, 2009.

[18] Hehre, W. J.; Ditchfie.R; Radom, L.; Pople, J. A., Molecular Orbital Theory of Electronic Structure of Organic Compounds .5. Molecular Theory of Bond Separation. J. Am. Chem. Soc. 1970, 92 (16), 4796-4801.

[19] Lalevee, J.; Allonas, X.; Fouassier, J. P., N-H and alpha(C-H) bond dissociation enthalpies of aliphatic amines. J. Am. Chem. Soc. 124: 9613-9621; 2002.

[20] Kaur, D.; Kaur, R. P., Evaluation of N-H bond dissociation energies in some amides using ab initio and density functional methods. J. Mol. Struc-Theochem. 757: 53-59; 2005.

[21] Viehe, H. G.; Janousek, Z.; Merenyi, R.; Stella, L., The Captodative Effect. Acc. Chem. Res. 18: 148-154; 1985.

[22] Chu, I. K.; Zhao, J.; Xu, M.; Siu, S. O.; Hopkinson, A. C.; Siu, K. W. M., Are the radical centers in peptide radical cations mobile? The generation, tautomerism, and dissociation of isomeric alpha-carbon-centered triglycine radical cations in the gas phase. J. Am. Chem. Soc. 2008, 130 (25), 7862-7872.

[23] Bagheri-Majdi, E.; Ke, Y. Y.; Orlova, G.; Chu, I. K.; Hopkinson, A. C.; Siu, K. W. M., Copper-mediated peptide radical ions in the gas phase. J. Phys. Chem. B 2004, 108 (30), 11170-11181.

[24] Ly, T.; Julian, R. R., Residue-specific radical-directed dissociation of whole proteins in the gas phase. J. Am. Chem. Soc. 130: 351-358; 2008.

[25] Scheraga, H. A.; Vila, J. V., J. A.; Arnautova, Y. A.; Vorobjev, Y., Assessing the fractions of tautomeric forms of the imidazole ring of histidine in proteins as a function of pH. Proc. Natl. Acad. Sci. USA 108: 5602-5607; 2011.

[26] Tanokura, M., H-1-Nmr Study on the Tautomerism of the Imidazole Ring of Histidine-Residues .1. Microscopic Pk Values and Molar Ratios of Tautomers in Histidine-Containing Peptides. Biochim. Biophys. Acta 742: 576-585; 1983.

[27] Diedrich, J. K.; Julian, R. R., Site-specific radical directed dissociation of peptides at phosphorylated residues. J. Am. Chem. Soc. 130: 12212-12213; 2008.

[28] Moore, B. N.; Blanksby, S. J.; Julian, R. R., Ion-molecule reactions reveal facile radical migration in peptides. Chem. Commun. 33: 5015-5017; 2009.

[29] Ly, T.; Zhang, X.; Sun, Q. Y.; Moore, B.; Tao, Y. Q.; Julian, R. R., Rapid, quantitative, and site specific synthesis of biomolecular radicals from a simple photocaged precursor. Chem. Commun. 47: 2835-2837; 2011.

Chapter 4

Ion Molecule Reactions Reveal Facile Radical Migration in Peptides

4.1 Introduction

With the continued development of mass spectrometric methods employing radical chemistry to fragment peptides and proteins in the gas phase, a detailed understanding of the behavior of radicals in gaseous peptide ions is vitally important. Numerous methods (including electron initiated fragmentation,[1,2] direct bond homolysis by photolysis[3] or collisional activation,[4-10] and photoionization[11]) can be used to generate peptide radicals. Following radical generation, the subsequent fragmentation chemistry of the peptide is typically dominated by radical-directed processes, making the location of the radical crucial as the initiation point for fragmentation. It is of paramount importance therefore, to determine whether radicals can migrate within the framework of a peptide or whether barriers exist to prevent such migration.

Recent work, based on the comparison of collisional activation mass spectra of isomeric triglycine radical peptides and accompanying electronic structure calculations, concluded that radical migration is restricted by substantial activation barriers.[12] In contrast, other computational studies have estimated

significantly smaller barriers.[13-15] In addition, a body of indirect experimental evidence also suggests that radical migration occurs in peptides prior to fragmentation.[16,17] However, experiments requiring collisional activation or other fragmentation methods are an imperfect probe of the structure of the nascent radical ions given that the possibility of radical migration (over substantial activation barriers), immediately prior to fragmentation, cannot be excluded. Herein, we demonstrate that reactive radicals generated within peptide cations can migrate immediately after their formation and without additional activation energy. This has been achieved through the novel combination of photodissociation for the regioselective generation of peptide radical cations and the use of ion-molecule reactions to probe the final location(s) of the radical.

Gas phase ion-molecule reactions have been used extensively in mass spectrometry as an alternative probe of molecular structure,[18] and have proven particularly powerful in differentiating isomeric radical ions.[19,20] Dioxygen has been shown to be a selective reagent, reacting with distonic radical ions (*i.e.*, where the charge and unpaired electron are formally localized on separate atoms within the molecule)[21-23] to form $[M+O_2]$ adduct ions while remaining unreactive toward conventional radical ions.[24-27] Furthermore, dioxygen is often present as a background gas inside commercial mass spectrometers thus obviating the need

for instrument modification to observe these ion-molecule reactions. In a recent example, McLuckey and co-workers found that peptide radical cations resulting from electron transfer dissociation of multiply charged polypeptides form $[M+O_2]$ adduct ions upon storage in an ion-trap mass spectrometer. This allows for the facile distinction between z-ions and their complementary even-electron c-ion counterparts.[28]

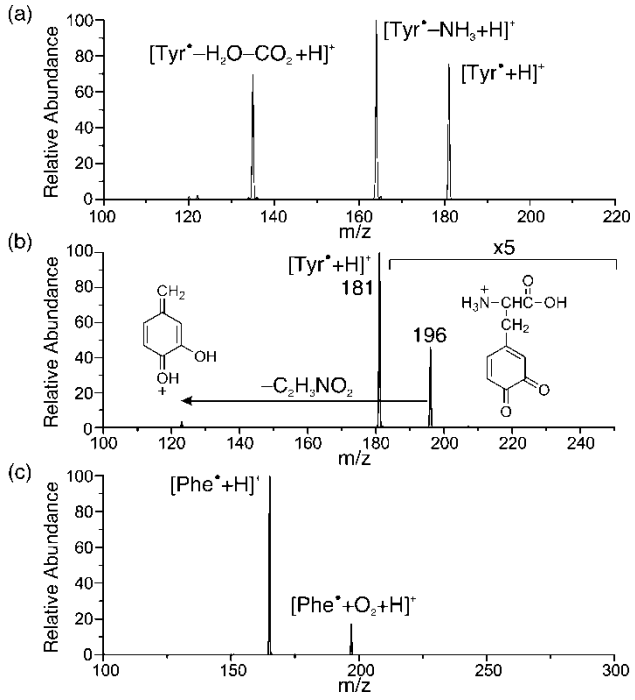

Figure 4.1 (a) Collision-induced dissociation mass spectrum of $[Tyr^{\bullet}+H]^+$. (b) The spectrum resulting from the gas phase reaction of $[Tyr^{\bullet}+H]^+$, formed via photodissociation (266 nm) of $[Tyr(I)+H]^+$, with O_2. (c) The spectrum resulting from the gas phase reaction of $[Phe^{\bullet}+H]^+$, formed via photodissociation (266 nm) of $[Phe(I)+H]^+$, with O_2.

4.2 Results and Discussion

We have previously demonstrated that peptide radical cations can be generated by the gas phase photodissociation of the C-I bond within iodinated tyrosine residues. Thus formed, these radicals yield site-specific fragmentation upon subsequent collisional activation. This method provides a known starting point for the radical at the 3-position of the tyrosine side chain. In this study, the archetypal tyrosinyl radical cation, $[Tyr^{\bullet}+H]^+$ (*m*/*z* 181), was generated by laser irradiation (266 nm) of protonated 3-iodotyrosine in a specially modified linear ion-trap mass spectrometer. The CID spectrum of $[Tyr^{\bullet}+H]^+$ (Figure 4.1a) shows neutral losses of 17 and 46 Da that have previously been assigned for the even-electron $[Tyr+H]^+$ cation to losses of NH_3 and $[CO+H_2O]$, respectively. [29,30] The absence of specific radical-driven dissociation products in Figure 4.1a is consistent with localisation of the unpaired electron at the 3-position on the phenyl moiety: with no evidence for radical migration even upon application of activation energy. Figure 4.1b shows the mass spectrum obtained from trapping $[Tyr^{\bullet}+H]^+$ in the presence of adventitious O_2 for 3 s. The absence of a significant $[M+O_2]^{\bullet+}$ adduct ion at *m*/*z* 213 contrasts with previous studies of distonic radical cations, as well as, the analogous reaction of O_2 with the phenylalaninyl radical cation, $[Phe^{\bullet}+H]^+$, formed *via* photolysis of protonated 4-iodophenylalanine

(Figure 4.1c). The presence of an abundant [M+15] ion in Figure 4.1b suggests distinctive reactivity for $[Tyr^{\bullet}+H]^{+}$ that can be rationalised in terms of addition of O_2 coupled with the elimination of $HO^{\bullet}$ facilitated by the adjacent hydroxyl group (Scheme 4.1).

This mechanism is supported by (i) the observation of the expected $DO^{\bullet}$ loss in the spectrum of the $[D_4\text{-}Tyr^{\bullet}+D]^{+}$ isotopologue and (ii) the retention of additional oxygen with the phenol moiety in the *m*/*z* 123 fragment ion formed by subsequent dissociation of the energized *m*/*z* 196 product ion (Figure 4.2a). Interestingly, the putative structure of the *m*/*z* 196 product ion corresponds to protonated dopaquinone: a reactive intermediate in the tyrosinase catalysed oxidation of tyrosine. [31,32] Taken together these data provide strong evidence for the localisation of the unpaired electron in the 3-position. Furthermore, kinetic analysis of the reaction of *m*/*z* 181 with dioxygen, yields strictly linear first-order kinetics with a second order rate constant of 6.2×10^{-12} molecules^{-1} cm^3 s^{-1} and a reaction efficiency of 1.1% (Figure 4.5a)**.** This behavior is indicative of a single, reactive radical cation at *m*/*z* 181 and we conclude that photodissociation of protonated 3-iodotyrosine at 266 nm yields a single phenyl-type radical structure that undergoes a distinctive concerted reaction in the presence of dioxygen as indicated in Scheme 4.1. The absence of exothermic rearrangements to stabilized

radicals (*e.g.*, phenoxyl, *a*- or *b*-radicals) suggests significant activation barriers exist for hydrogen atom transfer within this isolated amino acid.

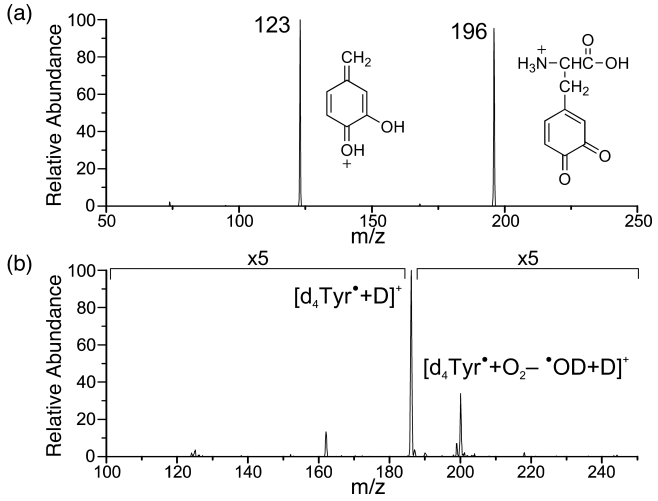

Figure 4.2 a) CID of $[Tyr^{\bullet} + O_2 + H]^+$ b) Gas phase reaction of $[d_4Tyr^{\bullet} + D]^+$ with O_2 for 3 seconds.

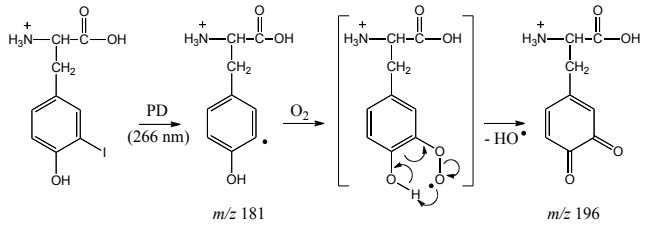

Scheme 4.1 Proposed mechanism for the reaction of $[Tyr^{\bullet}+H]^+$ with dioxygen.

The hexapeptide radical cation $[RGY^{\bullet}ALG+H]^+$ was synthesized *via* photodissociation of the 3-iodotyrosine analog. Figure 4.3a shows the mass spectrum obtained when this ion is trapped in the presence of O_2 for a period of 3 seconds. Significantly, in this spectrum the distinctive $[M+O_2\text{-}HO^{\bullet}]^+$ is of low abundance, suggesting few, if any, of these ions retain the radical in the 3-position on tyrosine. Furthermore, the observation of the $[M+O_2]^{\bullet+}$ adduct ion at

m/*z* 667 indicates the presence of an alternative reactive isomer in the radical ion population. Collision-induced dissociation of the $[RGYALG+H+O_2]^{\bullet+}$ at *m*/*z* 667 yields *m*/*z* 650, indicative of $HO^{\bullet}$ loss, while deuterium labeling of this peptide at the *a*-carbon on leucine results in $DO^{\bullet}$ loss under the same experimental conditions (Figure 4.4b). This suggests that the *m*/*z* 667 ion includes a peroxyl radical at leucine, resulting from migration of the radical to this residue *prior* to the reaction with O_2 (*cf*. Scheme 4.3). While these data indicate radical migration to leucine, the presence of other isomers resulting from rearrangement of the nascent radical cation cannot be excluded. Indeed, pseudo-first order kinetic analysis of the reaction of $[RGYALG+H]^{\bullet+}$ with dioxygen reveals significant curvature suggesting the ion population consists of at least two isomeric radical cations (Figure 4.5b); (i) a fast reacting radical with the unpaired electron likely localized on the leucine side-chain and (ii) a slow or unreactive isomer. Radical migration from the 3-positon on tyrosine to any of the *a*-position(s) along the peptide backbone is predicted to be exothermic by as much as 30 kcal mol^{-1}.[33] Such radicals may account for the less reactive fraction of the $[RGYALG+H]^{\bullet+}$ ion population. Indeed, the authentic *a*-radicals (at least initially), formed by collision-induced side-chain cleavage, are substantially less reactive or unreactive with O_2 (Figure 4.7).

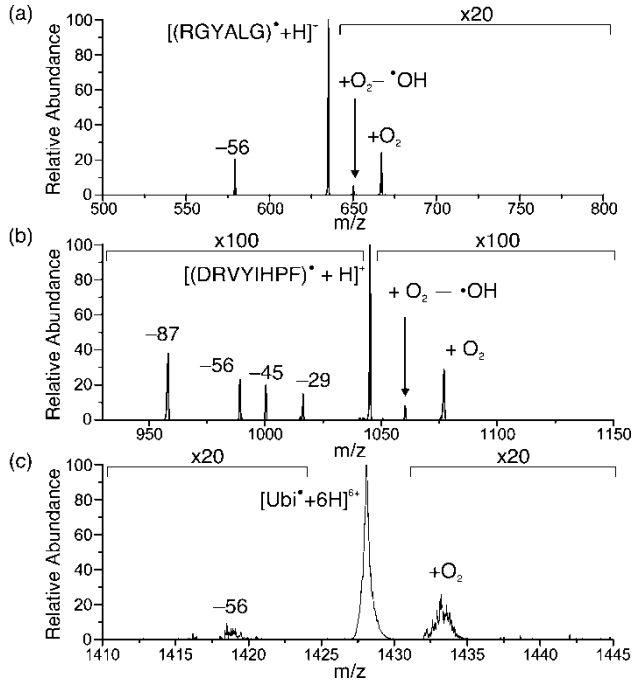

Figure 4.3 (a) The spectrum resulting from the gas phase reaction of $[RGYALG+H]^{\bullet+}$, formed via photodissociation (266 nm) of $[RGY(I)ALG+H]^{+}$, with O_2. The analogous spectra for the radical cations (b) $[DRVYIHPF+H]^{\bullet+}$ and (c) $[Ubiquitin+6H]^{\bullet 6+}$.

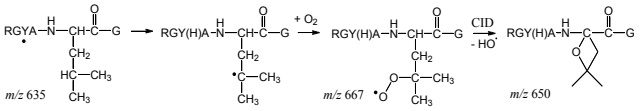

Scheme 4.2 Proposed mechanism for the reaction of $[RGYAL^{\bullet}G+H]^{+}$ with dioxygen.

We conclude therefore that following photodissociation of the C-I bond on the iodinated tyrosine residue, the radical does not remain localized at the 3-position but rather migrates to one or more locations throughout the peptide. Similar behavior is observed for the reaction of the angiotensin radical cation

[DRVYIHPF+H]$^{\bullet+}$ (Figures 4.3b) and even for multiply charged Ubiquitin (Figure 4.3c). The presence of $[M+O_2]^+$ adduct ions in these spectra is indicative of the presence of radicals at sites remote from the initial location on tyrosine.

Interestingly, the spectra shown in Figures 4.3 also reveal significant amounts of side-chain fragmentation similar to pathways previously described for the CID of peptide radicals,[39] *e.g.*, the loss of the isobutene (-56 Da) from the Leucine side-chain in Figure 4.3a. Furthermore, these fragmentation pathways reveal a time-dependence (Figure 4.6) and appear to be independent of the concentration of dioxygen (the latter was established by comparing the [RGYALG+O_2]$^{\bullet+}$ and [RGYALG-56]$^{\bullet+}$ ion abundances while varying the availability of air in the electrospray source region). These observations suggest that fast migration of the radical away from the tyrosine residue may be followed by subsequent slow unimolecular rearrangements some of which give rise to side-chain fragmentation.

4.3 Conclusion

The results presented herein unambiguously demonstrate that radical migration can occur in large peptides without the addition of significant activation energy. The possibility for facile radical migration must therefore be considered in fragmentation experiments where radical peptides are generated.

If needed, ion molecule reactions such as those demonstrated above can provide a facile route to monitor radical migration in peptides.

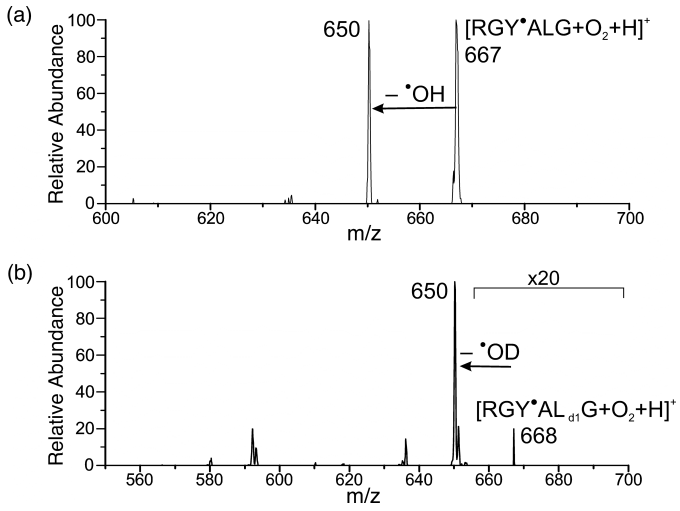

Figure 4.4 a) CID of $[RGY^{\bullet}ALG + O_2 + H]^+$ and b) CID of $[RGY^{\bullet}AL_{d1(\alpha)}G + O_2 + H]^+$

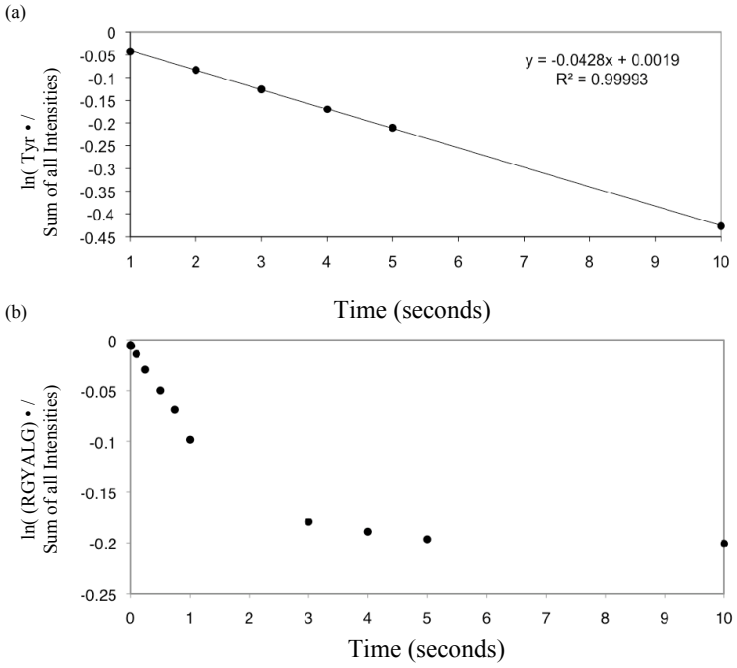

Figure 4.5 a) Kinetics plot of the reaction of $[Tyr^{\bullet} + H]^+$ with O_2 b) Kinetics plot of the reaction of $[(RGYALG)^{\bullet} + H]^+$ with O_2

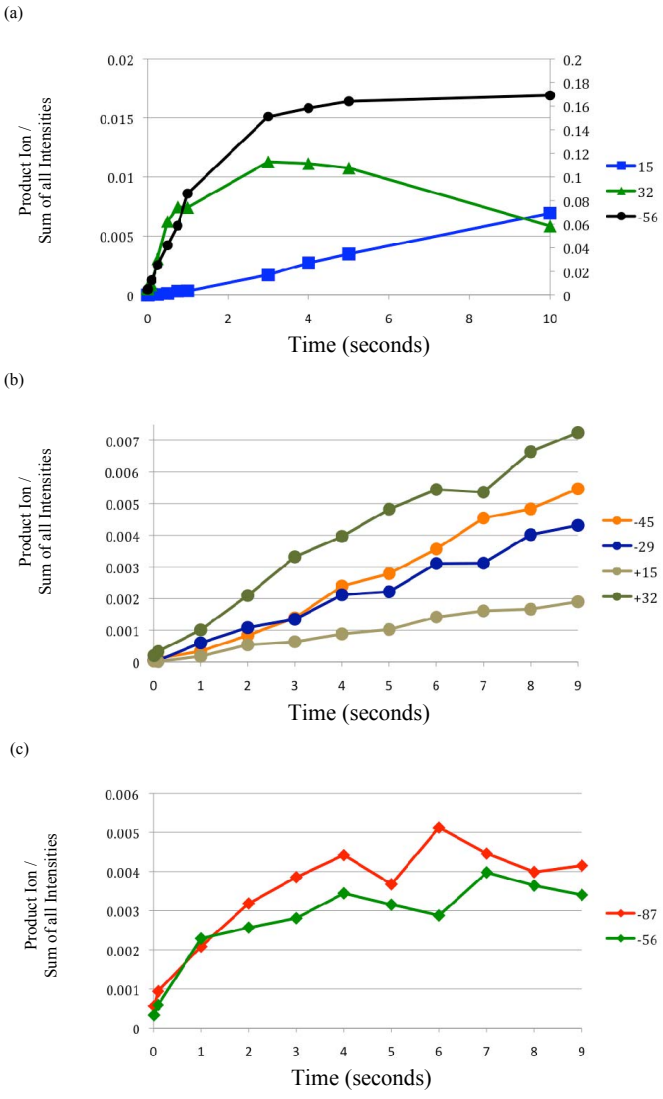

Figure 4.6 a) Kinetic plot of [(RGYALG)• + H]+ products. b) Kinetic plot of [(DRVYIHPF)• + H]+ linear products. c) Kinetic plot of [(DRVYIHPF)• + H]+ non-linear products.

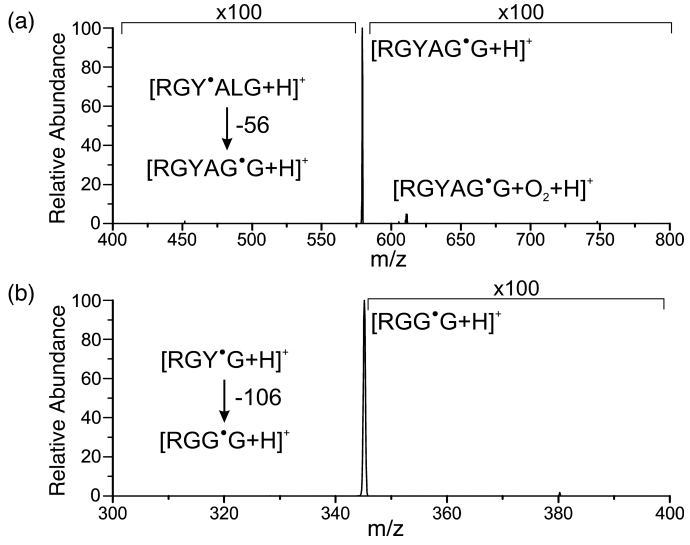

Figure 4.7 a) Gas phase reaction of $[RGYAG^{\bullet}G + H]^+$ with O_2 for 5 seconds. b) Gas phase reaction of $[RGG^{\bullet}G + H]^+$ with O_2 for 3 seconds.

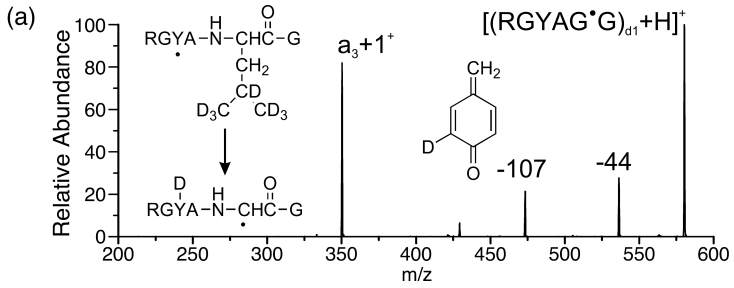

Figure 4.8 a) CID of $[(RGYAG^{\bullet}G)_{d1} + H]^+$ formed by trapping $[RGY^{\bullet}AL_{d7}G+H]^+$ for 3 seconds, then isolating the -62 Da sidechain loss product.

---

[1] J. E. P. Syka, J. J. Coon, M. J. Schroeder, J. Shabanowitz, D. F. Hunt, *Proc. Natl. Acad. Sci. U. S. A.* **2004**, *101*, 9528-9533.

[2] R. A. Zubarev, N. L. Kelleher, F. W. McLafferty, *J. Am. Chem. Soc.* **1998**, *120*, 3265-3266.

[3] T. Ly, R. R. Julian, *J. Am. Chem. Soc.* **2008**, *130*, 351-358.

[4] R. Hodyss, H. A. Cox, J. L. Beauchamp, *J. Am. Chem. Soc.* **2005**, *127*, 12436-12437.

[5] D. S. Masterson, H. Y. Yin, A. Chacon, D. L. Hachey, J. L. Norris, N. A. Porter, *J. Am. Chem. Soc.* **2004**, *126*, 720-721.

[6] S. Wee, A. Mortimer, D. Moran, A. Wright, C. K. Barlow, R. A. J. O'Hair, L. Radom, C. J. Easton, *Chem. Commun.* **2006**, 4233-4235.

[7] J. Laskin, Z. B. Yang, C. Lam, I. K. Chu, *Anal. Chem.* **2007**, *79*, 6607-6614.

[8] C. K. Barlow, S. Wee, W. D. McFadyen, R. A. J. O'Hair, *J. Chem. Soc., Dalton Trans.* **2004**, 3199-3204.

[9] I. K. Chu, T. Shoeib, X. Guo, C. F. Rodriquez, T. C. Lan, A. C. Hopkinson, K. W. M. Siu, *J. Am. Soc. Mass. Spectrom.* **2001**, *12*, 163-175.
[10] I. K. Chu, C. F. Rodriguez, F. Rodriguez, A. C. Hopkinson, K. W. M. Siu, *J. Am. Soc. Mass. Spectrom.* **2001**, *12*, 1114-1119.
[11] C. L. Kalcic, T. C. Gunaratne, A. D. Jones, M. Dantus, G. E. Reid *J. Am. Chem. Soc.*, Articles ASAP DOI: 10.1021/ja8089119
[12] I. K. Chu, J. Zhao, M. Xu, S. O. Siu, A. C. Hopkinson, K. W. M. Siu, *J. Am. Chem. Soc.* **2008**, *130*, 7862-7872.
[13] S.Panja, S. B. Nielsen, P. Hvelplund, F. Turecek, *J. Am. Soc. Mass Spectrom.* **2008**, *19*, 1726-1742.
[14] L. Jing, J. J. Nash, H. I. Kenttamaa, *J. Am. Chem. Soc.* **2008**, *130*, 17697-17709.
[15] F. Turecek, E. A. Syrstad, *J. Am. Chem. Soc.* **2003**, *125*, 3353-3369.
[16] N. Leymarie, C. E. Costello, P. B. O'Connor, *J. Am. Chem. Soc.* **2003**, *125*, 8949-8958.
[17] M. M. Savitski, F. Kjeldsen, M. L. Nielsen, R. A. Zubarev, *J. Am. Soc. Mass Spectrom.* **2007**, *18*, 113-120.
[18] M. N. Eberlin, *J. Mass Spectrom.* **2006**, *41*, 141-156.
[19] K. M. Stirk, L. K. M. Kiminkinen, H. I. Kenttämaa, *Chem. Rev.* **1992**, *92*, 1649-1665.
[20] H. Kenttämaa, in *Encyclopedia of Mass Spectrometry, Vol. 4* (Ed.: N. M. M. Nibbering), Elsevier, Amsterdam, **2005**, pp. 160-164.
[21] D. M. Tomazela, A. A. Sabino, R. Sparrapan, F. C. Gozzo, M. N. Eberlin, *J. Am. Soc. Mass. Spectrom.* **2006**, *17*, 1014-1022.
[22] B. F. Yates, W. J. Bouma, L. Radom, *Tetrahedron* **1986**, *42*, 6225-6234.
[23] B. F. Yates, W. J. Bouma, L. Radom, *J. Am. Chem. Soc.* **1984**, *106*, 5805-5808.
[24] D. G. Harman, S. J. Blanksby, *Org. Biomol. Chem.* **2007**, *5*, 3495-3503.
[25] D. G. Harman, S. J. Blanksby, *Chem. Commun.* **2006**, *8*, 859-861.
[26] A. Sorrilha, F. C. Gozzo, R. S. Pimpim, M. N. Eberlin, *J. Am. Soc. Mass. Spectrom.* **1996**, *7*, 1126-1137.
[27] S. J. Yu, C. L. Holliman, D. L. Rempel, M. L. Gross, *J. Am. Chem. Soc.* **1993**, *115*, 9676-9682.
[28] Y. Xia, P. A. Chrisman, S. J. Pitteri, D. E. Erickson, S. A. McLuckey, *J. Am. Chem. Soc.* **2006**, *128*, 11792-11798.
[29] J. F. Zhao, T. Shoeib, K. W. M. Siu, A. C. Hopkinson, *Int. J. Mass Spectrom.* **2006**, *255*, 265-278.
[30] H. Lioe, R. A. J. O'Hair, *Org. Biomol. Chem.* **2005**, *3*, 3618-3628.
[31] E. I. Solomon, U. M. Sundaram, T. E. Machonkin, *Chem. Rev.* **1996**, *96*, 2563-2605.
[32] T. Inoue, Y. Shiota, K. Yoshizawa, *J. Am. Chem. Soc.* **2008**, *130*, 16890-16897.
[33] Q. Sun, H. Nelson, T. Ly, B. M. Stoltz, R. R. Julian, *J. Prot. Res.* **2009,** *8* (2), 958-966.

Chapter 5

Dissociation Chemistry of Hydrogen Deficient Radical Peptide Anions

5.1 Introduction

Positively charged ions receive the majority of the attention from the mass spectrometric community when it comes to investigating peptides and proteins. Nevertheless, there are important reasons not to ignore anions. For one, many peptides prefer to adopt a negatively charged state. Take for example the synuclein proteins, which are associated with Parkinson's disease and some forms of cancer, and are dominated by acidic residues.[1,2] Furthermore, some important post-translational modifications such as phosphorylation, can also lead to preferential ionization as anionic species.[3] There are also important chemical differences between anions and cations. Most positively charged species are protonated, and dissociation following collisional activation is best explained in terms of the mobile proton model.[4] The absence of mobile protons in anionic peptides is therefore expected to substantially influence the dissociation chemistry. In contrast, most anionic species are deprotonated, with excess electrons serving as the charge carriers. Consequently, detachment of an electron following absorption of a photon occurs much more easily for anions than for

cations, which can also potentially influence the resulting dissociation that will be observed.[5]

Anionic peptides have been characterized to a limited extent by numerous methods including: collisional activation,[6] electron detachment,[7] electron capture,[8] action spectroscopy[9], and photoelectron spectroscopy.[10] Collisional activation has been the most commonly implemented approach and has been reviewed.[11] Electron detachment can be carried out by both photoactivation and via bombardment with high energy electrons.[12] The overall process leads to conversion of $[M\text{-}nH]^{n-}$ to $[(M\text{-}nH)\bullet]^{(n-1)-}$, creating a hydrogen deficient radical peptide (a peptide with one less hydrogen atom than its even electron counterpart). Electron capture, or the addition of another electron to a negatively charged peptide, is counterintuitive (but possible) and leads to the creation of a hydrogen abundant radical which exhibits distinct chemistry.[13] Action spectroscopy in the infrared can be utilized for structural evaluation for peptides of known primary sequence.

Radical directed dissociation (RDD) based methods have enabled unique capabilities for the characterization of peptides and proteins. For example, fragmentation can be directed to particular residues in selected cases.[14,15] Protein structure can be investigated by monitoring the degree of migration from a

specific radical initiation point.[16] The fragmentation pathways and chemistry of positively charged hydrogen deficient radicals have been studied extensively.[17-24] Hydrogen deficient radical anions have been neglected by comparison.[25,26] Interestingly, RDD is not a charge dominated process, in contrast with most other gas phase chemistry. The primary competition with RDD in positively charged peptides occurs when fully mobile protons exist, creating alternative low energy dissociation channels.[27-30] The absence of mobile protons is therefore potentially significant for RDD in anionic peptides.

It demonstrated herein that the fragmentation of hydrogen deficient deprotonated radical peptides is dominated by odd electron chemistry. For singly deprotonated species, RDD fragments including a, z, and c ions, accompanied by various side chain losses are primarily observed. Competitive b and y ion formation, typical of collisional activation for even electron ions, is not detected. Both of these observations suggest that charges do not play a critical role in defining the fragmentation of radical species. Photoactivation of multiply deprotonated anions generates radical species by both loss of iodine, following homolytic cleavage of a carbon-iodine bond, and by electron detachment. Interestingly, collisional activation of the radical following loss of iodine can lead to electron detachment as well. It was also determined that collisional activation

of deprotonated peptides with carbon-iodine bonds can be used to site specifically generate radical species, which has not been observed in protonated systems.

5.2 Experimental Methods

5.2.1 Chemicals and Reagents

The following peptides were purchased from American Peptide Company (Sunnyvale, CA): ADLIAYL-NH_2, DRLYSFGL-NH_2, GDGRLYAFGL-NH_2, DRVYIHP, YADFVVG-NH_2, AEAEYEK, SAEEYEYPS, SQNYPIV, VEPIPY, YPFVEPI, YEVHHQKLVFF, TRSAW, KWDNQ, KNRWEDPGKQLYNVEA, Ac-LMDKEAVYFAHLDIIW, SYSMEHFRWGKPVG, YGGFMRRVGRPEWWMDYQ, YMDGTMSQV. The peptide RGYDARA-NH_2 was synthesized by solid phase peptide synthesis. Sodium iodide (NaI), chloramine-T, sodium metabisulfite ($Na_2S_2O_5$) for peptide iodination and all the solvents used in the mass spectrometry experiments were purchased from Fisher Scientific (Fairlawn, NJ). Water was purified to 18.2 MΩ resistivity by a Millipore Direct-Q (Millipore, Billerica, MA) prior to use.

5.2.2 Preparation of Iodinated Peptides

To synthesize iodinated peptides, 10μL of a 1mM peptide stock solution (10nmol) was added to a 1.5mL eppendorf test tube containing 90μL H_2O and

10nmol NaI. To this, 1μL of 10mM chloramine-T stock solution (10nmol) was added and the test tube was allowed to sit in the dark for 1min. Finally, 15nmol $Na_2S_2O_5$ (1.5μL of the 10mM stock solution) was quickly spiked into the peptide solution and mixed well to quench the iodination reaction. This resulted in addition of a single iodine to tyrosine in roughly 50% yield. When not quenched, the reaction continues to completion to yield a statistical distribution of singly and multiply iodinated products with a maximum of two iodines added per tyrosine.

5.2.3 Photodissociation/Collision Induced Dissociation (PD/CID) of Iodinated Peptides

Aqueous iodinated peptide solutions (0.1mM) obtained from iodination reactions were first diluted to 10μM using 50/50 H_2O/ACN containing 50μM ammonium acetate. The dilute iodinated peptide solutions were directly infused into an LTQ linear ion trap mass spectrometer (Thermo Fisher Scientific, Waltham, MA) with a standard ESI source. The electrospray mode was switched between the positive and negative mode to acquire both cationic and anionic peptide ionization and fragmentation. To perform photodissociation (PD) with the LTQ linear ion trap mass spectrometer, the posterior plate of the LTQ was modified with a quartz window to transmit fourth harmonic (266nm) laser pulses from a flash lamp pumped Nd/YAG laser (Continuum, Santa Clara, CA).

The pulses were synchronized to the end of the isolation step of a typical MS^2 experiment by sending a TTL trigger signal from the mass spectrometer to the laser by a digital delay generator (Berkeley Nucleonics, San Rafael, CA). The anionic monoiodinated peptide ions were isolated for PD experiments. Further MS^3 experiments were performed by re-isolation of peptide radicals followed by collisional activation. The isolation window width of MS^2 and MS^3 experiments was limited to 5 Da. The collisional energy was optimized to deplete approximately 75% of the original precursor ion.

In regards to nomenclature, 'M' will be used to describe a molecule or peptide in its natural state. This does not include addition of protons or any chemical modification, i.e. iodination, and assumes an even electron species. Iodinated molecules will be represented with a preceding superscripted label, '^{I}M'. For protonated peptides, $[M+nH]^{n+}$ will be used to denote that 'n' protons have been added to the peptide. Similarly, $[M-nH]^{n-}$ indicates a loss of 'n' protons to generate anionic peptides. The creation of radical species by homolytically cleaving a chemical bond via photodissocation is used extensively throughout the manuscript. These radicals are generated independent of charge carrier, location, or polarity and are written in a form to reflect their distonic nature, i.e. $[M^{\bullet}+nH]^{n+}$ or $[M^{\bullet}-nH]^{n-}$. Importantly, generation of radicals by this method *does*

not affect the number of protons or charges present in the molecule. Photodetachment is also used to create radicals and *does* lead to changes in charge state. Photodetachment of an electron from an anionic peptide decreases the charge state, and is accompanied by the formation of a distonic radical. For example, photodetachment of an electron from $[M-2H]^{2-}$ would produce $[M^{\bullet}-2H]^{-}$ (note that the number of protons lost and charge state do not match in this case). Finally, both photodissociation and photodetachment can occur for some multiply charged anionic peptides. An example of this would be an iodinated peptide, $[^{I}M-2H]^{2-}$, undergoing photodissociation to form $[M^{\bullet}-2H]^{2-}$ followed by photodetachment to form $[M^{\bullet\bullet}-2H]^{-}$. This nomenclature indicates the initial presence of a diradical, although radical-radical recombination may subsequently occur as indicated in the text.

We will adopt the positive ion nomenclature to describe fragments in this manuscript. No structures are implied. The nomenclature is simply used to locate the point of fragmentation and convey whether the charge is on the C-terminus or N-terminus. This is appropriate, as recent careful studies have demonstrated that isobaric fragment ions do not unambiguously have the same structure (i.e. b ions are not all the same).[31,32]

5.2.4 Bond Dissociation Energy (BDE) Calculations

DFT calculations were performed at the B3LYP/6-31G(d) level of theory using Gaussian 09 Rev. A.1 (Gaussian, Inc., Wallingford, CT). All BDEs were determined by the isodesmic reaction method where each amino acid was extended on the N-terminus by a carbonyl group and on the C-terminus by an amine. The N-terminus was modeled as an alanine residue extended on the C-terminal side by an amine only. The backbone amide N-H was modeled by the dipeptide Ala-Ala. In the determination of beta carbon C-H BDEs, appropriate small molecules with experimentally known BDEs were chosen as references as previously described.[37] In addition, $(CH_3)_3CN$-H, C_6H_5-H, and $HCONHCH_3$ were chosen as reference molecules to accurately model the BDEs of the amine N-H, tyrosyl C-H, and amide N-H radicals respectively.[33-35]

5.3 Results and Discussion

The peptide SAEEYEYPS represents the C-terminal section of procholecystokinin, can be sulfated at both tyrosine residues, and helps regulate satiety.[36] SAEEYEYPS contains three acidic residues, no basic residues, and is easily observed when electrosprayed as a negatively charged ion. Mono-iodination leads to modification at either Tyr5 or Tyr7, roughly in equal abundance. The photodissociation (PD) spectrum generated by exposure to

266nm light for the singly deprotonated iodinated peptide is shown in Figure 5.1a. The primary product is the loss of iodine via homolytic cleavage, generating a hydrogen deficient radical. Some secondary dissociation is also observed, yielding a c_8 ion. Importantly, photodetachment of the electron does not appear to be a dominant process in Figure 5.1a (the ion count does not change significantly after the laser fires). Collisional activation of the peptide radical following loss of iodine and re-isolation is shown in Figure 1b. Abundant sidechain dissociation at tyrosine and glutamic acid is observed. The generation of a-type fragments at both tyrosine residues is consistent with a favorable dissociation pathway described previously.[37] Similarly, dissociation on the N-terminal side of serine to produce a c-ion has been described previously. Most of the fragmentation is therefore consistent with previous RDD experiments. However, the z_8 ion is not expected based on previously described mechanisms and will be discussed in further detail below. The loss of water is also dominant in Figure 5.1b, although this loss is not likely to occur via a radical directed mechanism. It has been noted previously that deprotonated peptides containing glutamic acid exhibit water loss.[11] With the exception of water loss, all other notable fragments appear to be generated via radical directed fragmentation mechanisms.

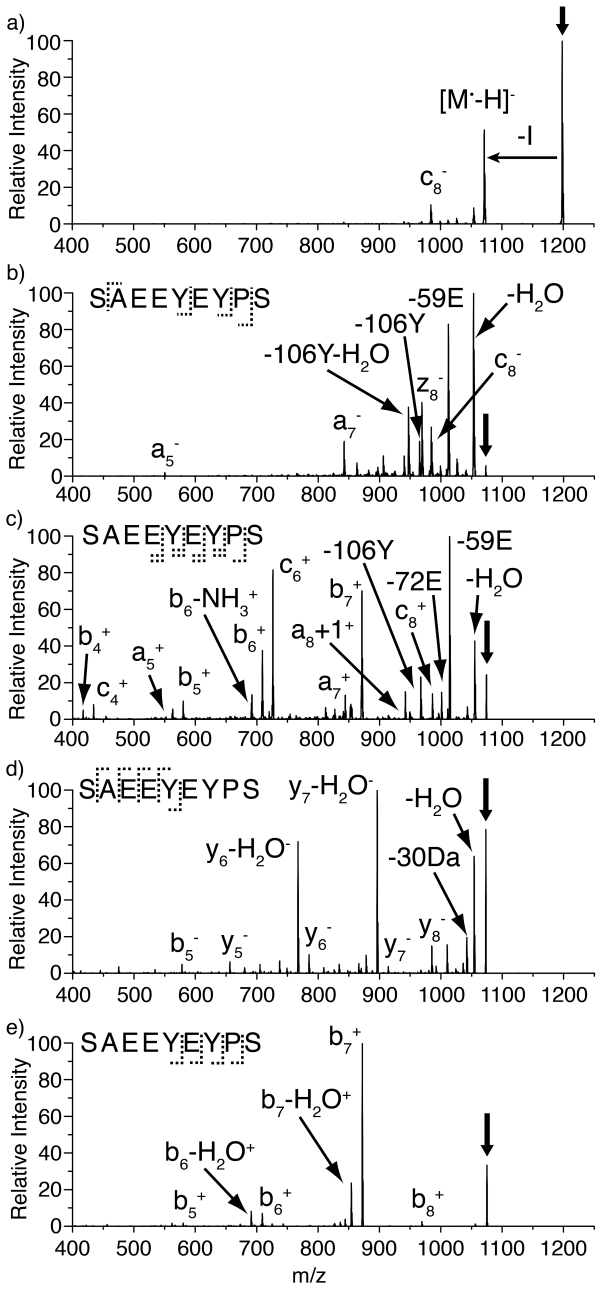

Figure 5.1 (a) PD of [ISAEEYEYPS-H]$^{-1}$. (b) CID of [SAEEYEYPS•-H]$^{-1}$. (c) CID of [SAEEYEYPS•+H]$^{+1}$. (d) CID of [SAEEYEYPS-H]$^{-1}$. (e) CID of [SAEEYEYPS+H]$^{+1}$. Bold downward arrows indicate precursor ion.

For comparison, the collisional activation of the equivalent protonated radical ion [SAEEYEYPS•+H]$^+$ is shown in Figure 5.1c. It is clear from the series of b ions which are observed that proton initiated dissociation pathways are competitive with RDD for the protonated peptide. Many of the RDD fragments are similar to those described in Figure 5.1b, although the z_8 fragment is notably absent. Finally, the CID spectra for the deprotonated and protonated even electron species are shown Figures 5.1d and 5.1e, respectively. With the exception of the loss of water, there are no substantial similarities between Figures 5.1b and 5.1d. This suggests that for anionic radical peptides, RDD accounts for the majority of the lowest energy dissociation pathways. In contrast, a sequence of b ions is observed in both Figures 5.1c and 5.1e, confirming that proton initiated dissociation is competitive with RDD when this peptide is protonated. The similarity observed in positive ion mode is consistent with previous results correlating high proton mobility with competitive proton-mediated dissociation.[27,28]

Shown in Figure 5.2 are CID spectra for deprotonated hydrogen deficient radicals of YEVHHQKLVFF (an Aβ fragment), ADLIAYL (a neuropeptide), and DRLYSFGL-NH_2 (an insect endocrine peptide). There are a variety of side chain losses which are observed (e.g. from Tyr, Leu, Arg, and Glu), which are

discussed collectively further below. Backbone fragmentation to yield a and z ions does not occur haphazardly, but is localized primarily to dissociation at aromatic residues which is consistent with known RDD mechanisms. There are very few b and y type ions, which are frequently observed following collisional activation of deprotonated peptides.[11] Taken as a whole, the data in Figures 5.1 and 5.2 suggests that RDD dissociation mechanisms for singly deprotonated peptides are largely similar to those described previously in relation to positively charge ions.[37] This observation is perhaps not surprising because no direct role is specified for the charge in any of the previous mechanisms.

Also observed in each spectrum in Figure 5.2 is a z-type fragment corresponding to loss of the N-terminal residue, as was also noted for SAEEYEYPS in Figure 5.1. The identities of the N-terminal and n+1 residues are different for each peptide, suggesting that the dissociation is likely a property of the N-terminus itself. A proposed mechanism to account for these z fragments is shown in Scheme 5.1. This mechanism begins with the radical located at the N-terminus. This is not unreasonable since the N-terminus has an N-H bond dissociation energy of 383 kJ/mol which is well below that of the initial tyrosyl radical (475 kJ/mol). Migration from the initial tyrosyl radical or from a variety of other potential intermediate sites to the N-terminus would therefore be predicted

to be exothermic. Dissociation beta to the initial radical eliminates the N-terminal residue and generates a radical x-type fragment. Radical x-ions are known to be unstable and frequently spontaneously lose HNCO to yield more stable z-type ions.

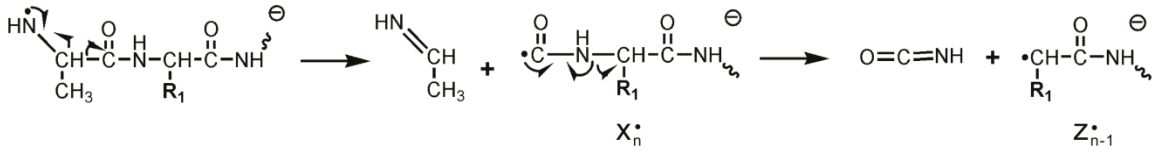

Scheme 5.1 Mechanism of formation of z_{n-1} ions by RDD.

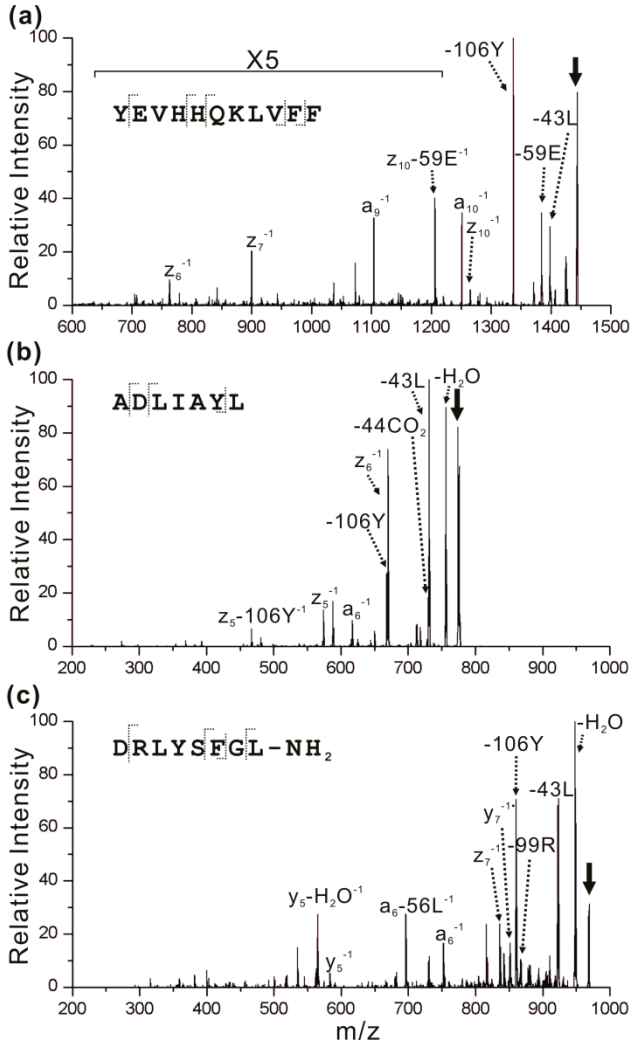

Figure 5.2 (a) CID of [YEVHHQKLVFF•-H]$^{-1}$. (b) CID of [ADLIAYL•-H]$^{-1}$. (c) CID of [DRLYSFGL–NH_2•-H]$^{-1}$. Bold downward arrows indicate precursor ion.

This mechanism was probed experimentally with TRSAW, a fragment of the parathyroid hormone related protein,[38] as shown in Figure 5.3. The radical peptides in Figure 5.3 were generated by noncovalent attachment of an iodonaphthyl 18-crown-6 based molecule as described previously.[37] Collisional activation of [TRSAW•+H]$^+$ yields primarily loss of CO_2 and an N-terminal z_4 ion,

which could be formed by the mechanism shown in Scheme 5.1. In Figure 5.3b, TRSAW has been acetylated, yielding a combination of acetylation at the N-terminus and at serine. Collisional activation yields a z_4 ion which retains the acetyl modification, indicating that acetylation of serine does not influence formation of this ion. However, no unmodified z_4 ion is detected, suggesting that acetylation at the N-terminus does interfere. According to Scheme 1, N-terminal acetylation would require abstraction of an amide hydrogen, which is significantly less energetically favorable than an amine hydrogen (BDEs of 453[35] and 383 kJ/mol, respectively). This explains the absence of the z_4 ion and also provides a rationale for why z ions are not generated throughout the peptide. In Figure 5.3b an unmodified z_5 ion is observed. This ion is created by threonine via a mechanism described previously[39] and confirms that the threonine side chain is not acetylated. The mechanism shown in Scheme 5.1 is again not directly related to charge or charge polarity; however, this pathway is affected if the N-terminus is protonated, which makes hydrogen abstraction significantly less energetically favorable.

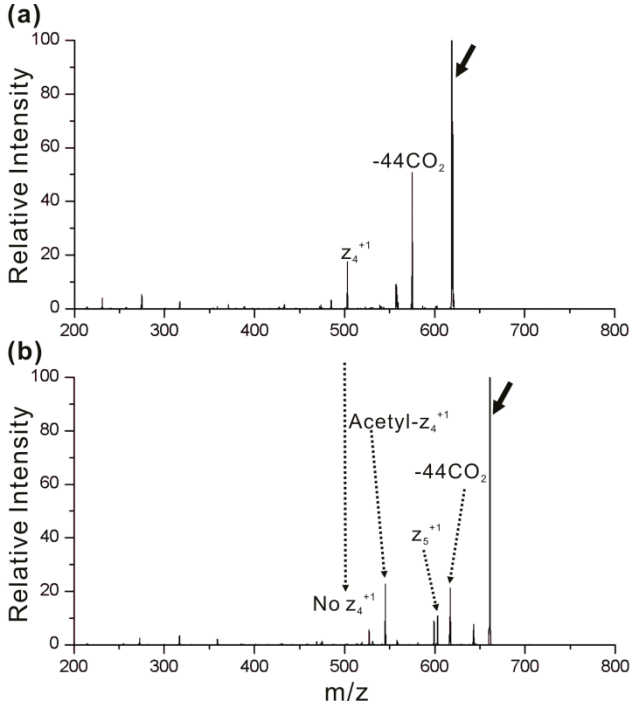

Figure 5.3 (a) CID of $[TRSAW^{\bullet}+H]^+$. (b) CID of mixture of $[Ac\text{-}TRSAW^{\bullet}+H]^+$ and $[TRAc\text{-}SAW^{\bullet}+H]^+$. Bold downward arrows indicate precursor ion.

General trends in dissociation observed for deprotonated hydrogen deficient peptide radicals are summarized in Figure 5.4 (the peptides are listed in the experimental section). Figure 5.4a plots the average relative abundance of backbone dissociation for each amino acid. Also shown are the BDEs for the β-hydrogens of each amino acid side chain, which is where backbone dissociation in RDD is typically initiated.[17] As can be seen from the data, lower BDEs (on average) correlate with increased yield of backbone dissociation. This is consistent with observations found previously for positively charged peptides.[37] Importantly, the BDEs only relate to the thermodynamics of radical migration,

and are therefore not expected to correlate quantitatively with the observed dissociation probabilities because kinetics will also play a role in the fragmentation of each peptide. The surprising degree of correlation in Figure 4a suggests that on average for these large molecules, the kinetics of radical migration are not generally dominant.

In Figure 5.4b, the relative abundances of side chain dissociation products are shown, with the average values represented as triangles. Individual values often cover the entire scale and range from no observable dissociation to being the most abundant side chain loss. This range is due to kinetic factors largely dictated by the particular structures for each peptide which favor or inhibit migration of the radical to a particular side chain. However, the averages are again revealing in terms of the thermodynamics of radical migration. For each side chain from which multiple dissociations are observed, the loss initiated from the site with a lower BDE[40] (which is always the smaller mass loss originating from a C_α radical e.g. -43 for Leu) is observed more frequently.

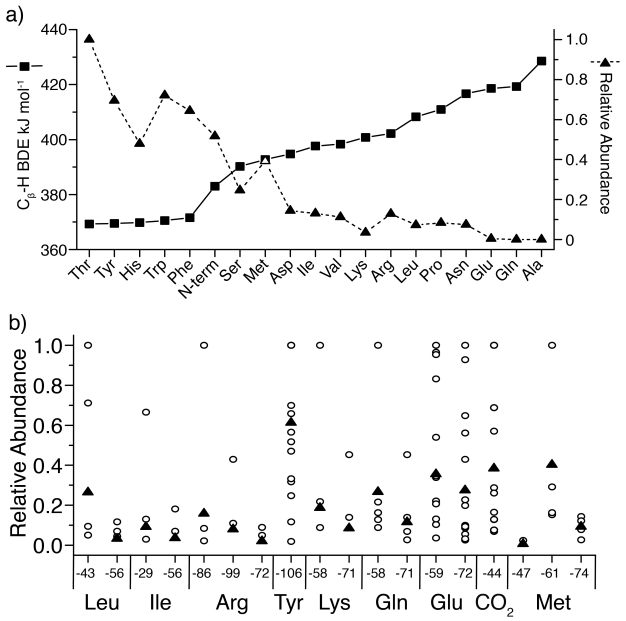

Figure 5.4 Statistical summary of data for all peptides listed in the Experimental section. (a) C_β-H bond dissociation energy (solid square) and normalized relative abundances of anionic radical induced backbone fragments (solid triangle); on average backbone fragmentation is favored at residues with low BDEs. (Note: Cys was not present in the peptides sampled.) (b) Propensities of side chain losses at each amino acid following collisional activation of peptide radical anion precursors. Open circles are individual experimentally observed side chain losses, solid triangles represent averaged values.

The photoactivation of multiply charged anions is explored in Figure 5.5. Photoactivation of triply deprotonated iodo-SAEEYEYPS is shown in Figure 5.5a. Several products are observed, all in fairly low abundance: loss of iodine, loss of an electron, loss of an electron and iodine, and loss of an electron and iodine and CO_2. Subsequent collisional activation of the loss of iodine product is shown in Figure 5.5b. Surprisingly, the primary product afforded by CID is electron detachment.[41,42] The electron affinities of the initial charge carrying groups (carboxylates) are quite high (>3.2eV)[43], suggesting that thermionic like emission

is unlikely from these groups. This is supported by the observation that electron detachment is not observed in collisional activation of deprotonated peptide anions. It is also possible that an electron could have been promoted into a weakly bound orbital following absorption of a photon, which is then lost upon collisional activation. However, it is not clear how this electron would survive the high pressure and electric fields present in an ion trap long enough to allow isolation and collisional activation. A third possibility would be radical attack of the carboxylate anion, leading to concurrent formation of a new covalent bond and electron detachment (see Scheme 5.2). The energy from bond formation could drive electron detachment in this scenario. Collisional activation of the product following electron detachment yields the spectrum shown in Figure 5.5c which is consistent with the type of crosslink that would be formed by the mechanism in Scheme 5.2. Further experiments will be required to definitively determine which of these possibilities actually leads to electron detachment.

Several additional minor side chain losses and backbone fragments consistent with RDD are also observed in Figure 5.5b. The loss of 71 Da corresponds to loss of the deprotonated glutamic acid side chain as shown in Scheme 5.3. A small y_8 ion is also present. This fragment would not be expected to occur via a radical directed process; however, it is consistent with a

crosslinked peptide generated after recombination of a diradical. The y_8 ion is the second most abundant product in Figure 5.5c, suggesting that the y_8 in Figure 5.5b likely results from subsequent fragmentation of hot $[SAEEYEYPS^{\bullet\bullet}\text{-}3H]^{-2}$ following loss of iodine and electron detachment.

Similar results are obtained for doubly deprotonated YPFVEPI (a casein related peptide) as shown in Figure 5.5d. Collisional activation of $[YPFVEPI^{\bullet}\text{-}2H]^{-2}$ (following loss of iodine) again leads primarily to electron detachment. Subsequent activation of the electron detached product yields almost exclusive loss of CO_2, which is again consistent with crosslinking following diradical recombination. In addition to electron detachment, loss of CO_2 and charged glutamic acid side chains are once again observed.

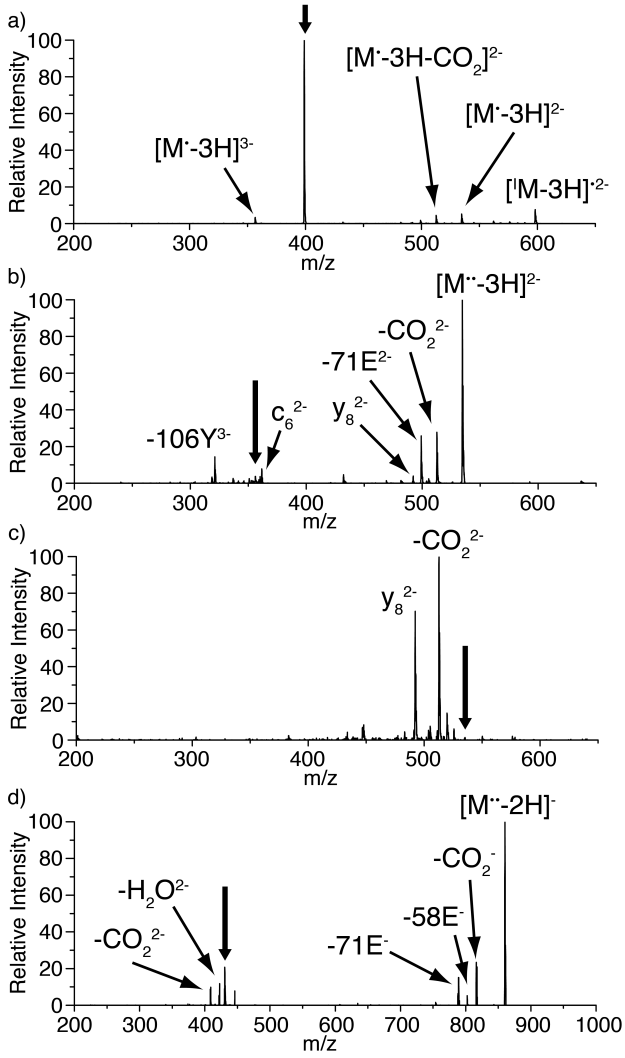

Figure 5.5 (a) PD of [ISAEEYEYPS-3H]$^{-3}$. (b) CID of [SAEEYEYPS•-3H]$^{-3}$. (c) CID of [SAEEYEYPS-3H]$^{-2}$. (d) CID of [YPFVEPI•-2H]$^{-2}$. Bold downward arrows indicate precursor ion.

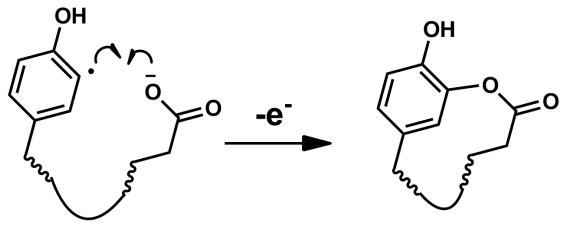

Scheme 5.2 Potential mechanism leading to electron detachment.

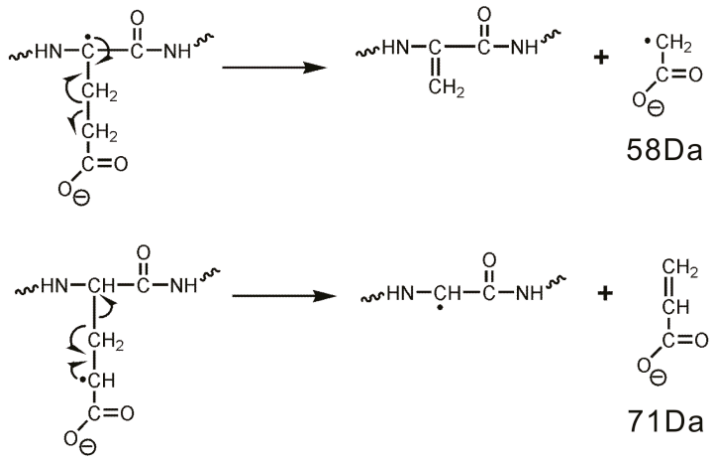

Scheme 5.3 Mechanism of side chain losses from deprotonated Glu.

PD can be utilized to generate radicals regardless of charge polarity; however, collisional activation of iodinated peptides in positive ion mode does not lead to loss of iodine and generation of hydrogen deficient radical species. Shown in Figure 5.6a is the CID spectrum for deprotonated ^{I}AEAEYEK (iodinated at tyrosine). Surprisingly, the largest peaks correspond to loss of iodine and loss of iodine with several side chains. Isolation of the loss of iodine peak followed by collisional activation is shown in Figure 5.6b. The corresponding spectrum where the radical was created by photoactivation is provided in Figure 5.6c. The two figures are very similar both in terms of product ion identity and intensity, suggesting that the method for creating the radical in this case does not significantly influence the results. The mechanism that leads to loss of iodine in anion mode is not fully understood; however, it is known that

the carbon-iodine bond is weak in comparison to naturally occurring bonds in peptides. It is possible that in the absence of proton catalyzed dissociation pathways, cleavage of this bond is simply one of the lowest energy dissociation routes.

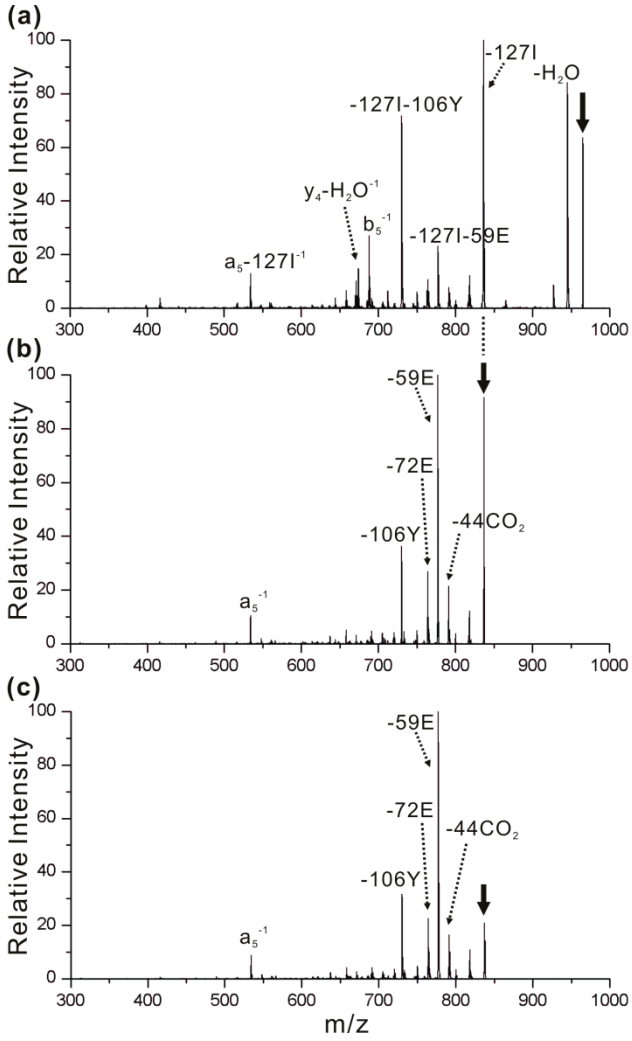

Figure 5.6 (a) CID of $[^{I}AEAEYEK\text{-}H]^{-1}$. (b) CID of $[AEAEYEK^{\bullet}\text{-}H]^{-1}$, radical generated by CID. (c) CID of $[AEAEYEK^{\bullet}\text{-}H]^{-1}$, radical generated by PD. Bold downward arrows indicate precursor ion.

5.4 Conclusions

Many of the radical chemistry dissociation pathways that occur in deprotonated peptides are very similar to those found in protonated peptides. In other words, the charges do not play a central mechanistic role in either case. However, there are also a variety of interesting and important differences which distinguish anionic peptides from their cationic counterparts. For example, the absence of competitive low energy proton initiated dissociation pathways in singly deprotonated radical peptides leads to dissociation dominated by radical chemistry. Similarly, the absence of protons favors backbone fragmentation at the N-terminal residue for anionic radical peptides via a mechanism which is inhibited if the N-terminus is protonated.

In the case of multiply deprotonated peptides, photoactivation at 266nm yields both fragmentation of carbon-iodine bonds and electron detachment (which is not observed in protonated systems). Interestingly, subsequent collisional activation of the hydrogen deficient radicals generated by PD also leads to a substantial amount of electron detachment. Such collision induced electron detachment has not been previously observed for any peptides or peptide radicals to the best of our knowledge. Similarly, collisional activation of deprotonated peptides can be leveraged to create hydrogen deficient radicals via

dissociation pathways yielding homolytic fragmentation of carbon-iodine bonds.

Analogous experiments with protonated peptides do not yield radical species.

---

[1] Wright, J. A.; Brown, D. R., Alpha-synuclein and its role in metal binding: Relevance to Parkinson's disease. *J. Neurosci. Res.* **2008,** *86* (3), 496-503.
[2] Ahmad, M.; Attoub, S.; Singh, M. N.; Martin, F. L.; El-Agnaf, O. M. A., gamma-synuclein and the progression of cancer. *Faseb Journal* **2007,** *21* (13), 3419-3430.
[3] Janek, K.; Wenschuh, H.; Bienert, M.; Krause, E., Phosphopeptide analysis by positive and negative ion matrix-assisted laser desorption/ionization mass spectrometry. *Rapid Commun. Mass Spectrom.* **2001,** *15* (17), 1593-1599.
[4] Dongre, A. R.; Jones, J. L.; Somogyi, A.; Wysocki, V. H., Influence of peptide composition, gas-phase basicity, and chemical modification on fragmentation efficiency: Evidence for the mobile proton model. *J. Am. Chem. Soc.* **1996,** *118* (35), 8365-8374.
[5] Larraillet, V.; Antoine, R.; Dugourd, P.; Lemoine, J., Activated-Electron Photodetachment Dissociation for the Structural Characterization of Protein Polyanions. *Anal. Chem.* **2009,** *81* (20), 8410-8416.
[6] Hu, P. F.; Gross, M. L., Gas-phase anionic complexes of alkali-metal ions and peptides - structure and collision-activated decompositions. *J. Am. Soc. Mass Spectrom.* **1994,** *5* (3), 137-143.
[7] Antoine, R.; Joly, L.; Tabarin, T.; Broyer, M.; Dugourd, P.; Lemoine, J., Photo-induced formation of radical anion peptides. Electron photodetachment dissociation experiments. *Rapid Commun. Mass Spectrom.* **2007,** *21* (2), 265-268.
[8] Song, H.; Hakansson, K. Improved negative ion electron capture dissociation from coupling with proton transfer reaction. *Proceedings of the 59th ASMS Conference on Mass Spectrometry and Allied Topics*, 2011.
[9] Oomens, J.; Steill, J. D., The Structure of Deprotonated Tri-Alanine and Its a(3)(-) Fragment Anion by IR Spectroscopy. *J. Am. Soc. Mass Spectrom.* **2010,** *21* (5), 698-706.
[10] Vonderach, M.; Ehrler, O. T.; Matheis, K.; Karpuschkin, T.; Papalazarou, E.; Brunet, C.; Antoine, R.; Weis, P.; Hampe, O.; Kappes, M. M.; Dugourd, P., Probing electrostatic interactions and structural changes in highly charged protein polyanions by conformer-selective photoelectron spectroscopy. *PCCP* **2011,** *13* (34), 15554-15558.
[11] Bowie, J. H.; Brinkworth, C. S.; Dua, S., Collision-induced fragmentations of the (M-H)(-) parent anions of underivatized peptides: An aid to structure determination and some unusual negative ion cleavages. *Mass Spectrometry Reviews* **2002,** *21* (2), 87-107.
[12] Kalli, A.; Hakansson, K., Preferential cleavage of S-S and C-S bonds in electron detachment dissociation and infrared multiphoton dissociation of disulfide-linked peptide anions. *Int. J. Mass Spectrom.* **2007,** *263* (1), 71-81.
[13] Yoo, H. J.; Wang, N.; Zhuang, S.; Song, H.; Hakansson, K., Negative-Ion Electron Capture

Dissociation: Radical-Driven Fragmentation of Charge-Increased Gaseous Peptide Anions. *J. Am. Chem. Soc.* **2011**.

[14] Diedrich, J. K.; Julian, R. R., Site-specific radical directed dissociation of peptides at phosphorylated residues. *J. Am. Chem. Soc.* **2008,** *130* (37), 12212.

[15] Diedrich, J. K.; Julian, R. R., Site-Selective Fragmentation of Peptides and Proteins at Quinone-Modified Cysteine Residues Investigated by ESI-MS. *Anal. Chem.* **2010,** *82* (10), 4006-4014.

[16] Ly, T.; Julian, R. R., Elucidating the Tertiary Structure of Protein Ions in Vacuo with Site Specific Photoinitiated Radical Reactions. *J. Am. Chem. Soc.* **2010,** *132* (25), 8602-8609.

[17] Ly, T.; Julian, R. R., Tracking Radical Migration in Large Hydrogen Deficient Peptides with Covalent Labels: Facile Movement does not Equal Indiscriminate Fragmentation. *J. Am. Soc. Mass Spectrom.* **2009,** *20* (6), 1148-1158.

[18] Moore, B. N.; Blanksby, S. J.; Julian, R. R., Ion-molecule reactions reveal facile radical migration in peptides. *Chem. Commun.* **2009,** (33), 5015-5017.

[19] Hodyss, R.; Cox, H. A.; Beauchamp, J. L., Bioconjugates for tunable peptide fragmentation: Free radical initiated peptide sequencing (FRIPS). *J. Am. Chem. Soc.* **2005,** *127* (36), 12436-12437.

[20] Chung, T. W.; Turecek, F., Backbone and Side-Chain Specific Dissociations of z Ions from Non-Tryptic Peptides. *J. Am. Soc. Mass Spectrom.* **2010,** *21* (8), 1279-1295.

[21] Yin, H.; Chacon, A.; Porter, N. A.; Yin, H. Y.; Masterson, D. S., Free radical-induced site-specific peptide cleavage in the gas phase: Low-energy collision-induced dissociation in ESI- and MALDI mass spectrometry. *J. Am. Soc. Mass Spectrom.* **2007,** *18* (5), 807-816.

[22] Wee, S.; O'Hair, R. A. J.; McFadyen, W. D., The role of the position of the basic residue in the generation and fragmentation of peptide radical cations. *Int. J. Mass Spectrom.* **2006,** *249*, 171-183.

[23] Laskin, J.; Futrell, J. H.; Chu, I. K., Is dissociation of peptide radical cations an ergodic process? *J. Am. Chem. Soc.* **2007,** *129* (31), 9598-+.

[24] Chu, I. K.; Rodriguez, C. F.; Rodriguez, F.; Hopkinson, A. C.; Siu, K. W. M., Formation of molecular radical cations of enkephalin derivatives via collision-induced dissociation of electrospray-generated copper (II) complex ions of amines and peptides. *J. Am. Soc. Mass. Spectrom.* **2001,** *12* (10), 1114-1119.

[25] Laskin, J.; Yang, Z. B.; Lam, C.; Chu, I. K., Charge-remote fragmentation of odd-electron peptide ions. *Anal. Chem.* **2007,** *79* (17), 6607-6614.

[26] Lam, C. N. W.; Chu, I. K., Formation of anionic peptide radicals in vacuo. *J. Am. Soc. Mass Spectrom.* **2006,** *17* (9), 1249-1257.

[27] Laskin, J.; Yang, Z. B.; Ng, C. M. D.; Chu, I. K., Fragmentation of alpha-Radical Cations of Arginine-Containing Peptides. *J. Am. Soc. Mass Spectrom.* **2010,** *21* (4), 511-521.

[28] Knudsen, E. R.; Julian, R. R., Fragmentation chemistry observed in hydrogen deficient radical peptides generated from N-nitrosotryptophan residues. *Int. J. Mass Spectrom.* **2010,** *294* (2-3), 83-87.
[29] Lam, A. K. Y.; Ryzhov, V.; O'Hair, R. A. J., Mobile Protons Versus Mobile Radicals: Gas-Phase Unimolecular Chemistry of Radical Cations of Cysteine-Containing Peptides. *J. Am. Soc. Mass Spectrom.* **2010,** *21* (8), 1296-1312.
[30] Xu, M. J.; Song, T.; Quan, Q. A.; Hao, Q. A.; Fang, D. C.; Siu, C. K.; Chu, I. K., Effect of the N-terminal basic residue on facile C(alpha)-C bond cleavages of aromatic-containing peptide radical cations. *Physical Chemistry Chemical Physics* **2011,** *13* (13), 5888-5896.
[31] Bythell, B. J.; Somogyi, A.; Paizs, B., What is the Structure of b(2) Ions Generated from Doubly Protonated Tryptic Peptides? *J. Am. Soc. Mass Spectrom.* **2009,** *20* (4), 618-624.
[32] Savitski, M. M.; Hith, M.; Fung, Y. M. E.; Adams, C. M.; Zubarev, R. A., Bifurcating Fragmentation Behavior of Gas-Phase Tryptic Peptide Dications in Collisional Activation. *J. Am. Soc. Mass Spectrom.* **2008,** *19* (12), 1755-1763.
[33] Lalevee, J.; Allonas, X.; Fouassier, J. P., N-H and alpha(C-H) bond dissociation enthalpies of aliphatic amines. *J. Am. Chem. Soc.* **2002**, *124* (32), 9613-9621.
[34] Blanksby, S. J.; Ellison, G. B., Bond dissociation energies of organic molecules. *Acc. Chem. Res.* **2003**, *36* (4), 255-263.
[35] Kaur, D.; Kaur, R. P., Evaluation of N-H bond dissociation energies in some amides using ab initio and density functional methods. *J. Mol. Struc-Theochem* **2005**, *757* (1-3), 53-59.
[36] Vishnuvardhan, D.; Beinfeld, M. C., Role of tyrosine sulfation and serine phosphorylation in the processing of procholecystokinin to amidated cholecystokinin and its secretion in transfected AtT-20 cells. *Biochemistry* **2000,** *39* (45), 13825-13830.
[37] Sun, Q. Y.; Nelson, H.; Ly, T.; Stoltz, B. M.; Julian, R. R., Side Chain Chemistry Mediates Backbone Fragmentation in Hydrogen Deficient Peptide Radicals. *J. Prot. Res.* **2009,** *8* (2), 958-966.
[38] Philbrick, W. M.; Wysolmerski, J. J.; Galbraith, S.; Holt, E.; Orloff, J. J.; Yang, K. H.; Vasavada, R. C.; Weir, E. C.; Broadus, A. E.; Stewart, A. F., Defining the roles of parathyroid hormone-related protein in normal physiology. *Physiol. Rev.* **1996,** *76* (1), 127-173.
[39] Moore, B. N.; Ly, T.; Julian, R. R., Radical Conversion and Migration in Electron Capture Dissociation. *J. Am. Chem. Soc.* **2011,** *133* (18), 6997-7006.
[40] Rauk, A.; Yu, D.; Taylor, J.; Shustov, G. V.; Block, D. A.; Armstrong, D. A., Effects of structure on C-alpha-H bond enthalpies of amino acid residues: Relevance to H transfers in enzyme mechanisms and in protein oxidation. *Biochemistry* **1999,** *38* (28), 9089-9096.
[41] Fu, Y. J.; Laskin, J.; Wang, L. S., Collision-induced dissociation of 4Fe-4S cubane cluster complexes: Fe4S4Cl4-x(SC2H5)(x) (2-/1-) (x=0-4). *Int. J. Mass Spectrom.* **2006,** *255*, 102-110.
[42] Simons, J., Propensity Rules for Vibration-Induced Electron Detachment of Anions. *J. Am. Chem. Soc.* **1981,** *103* (14), 3971-3976.

[43] Lu, Z.; Continetti, R. E., Dynamics of the acetyloxyl radical studied by dissociative photodetachment of the acetate anion. *J. Phys. Chem. A* **2004,** *108* (45), 9962-9969.

Chapter 6

Concluding Remarks

6.1 Overview

Radical chemistry is a powerful tool for the manipulation of covalent bonds. In this dissertation, gas phase radical chemistry in peptides and proteins was explored in detail. Fragmentation patterns in ECD, ETD, and RDD were shown to be related due to their dependence on radical chemistry. Radical migration by hydrogen abstraction was examined as the primary method of intramolecular radical transfer in peptides and proteins. The thermodynamic factors controlling this process were examined by quantum mechanical calculation and compared to experimentally observed fragmentation patterns in anionic peptides and results from ion-molecule reactions. The experimental results were in agreement with what was predicted by calculation.

6.2 Future Directions

There are numerous unexplored uses of radical chemistry in mass spectrometry. For peptide radicals in particular, the key to unlocking much of this potential lies in the exploration of new chemical modifications. This work has led to a deeper understanding of BDEs and radical migration in peptides.

The future direction now is to leverage this knowledge into experiments designed to examine protein structure, sequence peptides, or identify specific PTMs. This will be possible by designing chemical modifications which modify or add on to the existing BDE landscape presented by peptides or proteins. The validity of this approach to influence the migration of radicals has been demonstrated in this work.

The utility of the BDEs and gas phase radical migration observations presented here may extend beyond mass spectrometry and be useful in the examination of solution phase biological systems. This information presented here may also be applicable outside of the peptide and protein arena. Investigation of small molecule or other biopolymer BDEs would be useful in determining what other radical reactions and migration pathways are possible in the cellular environment. Significant progress in the examination of radicals in biological systems will be attained from capitalizing on the knowledge presented in this work. In general, increased understanding of the factors that control the behavior of radicals has the potential to open up new avenues of research in the field.